SCHOOL OF
PHYSICAL SCIENCES
AND NANOTECHNOLOGY

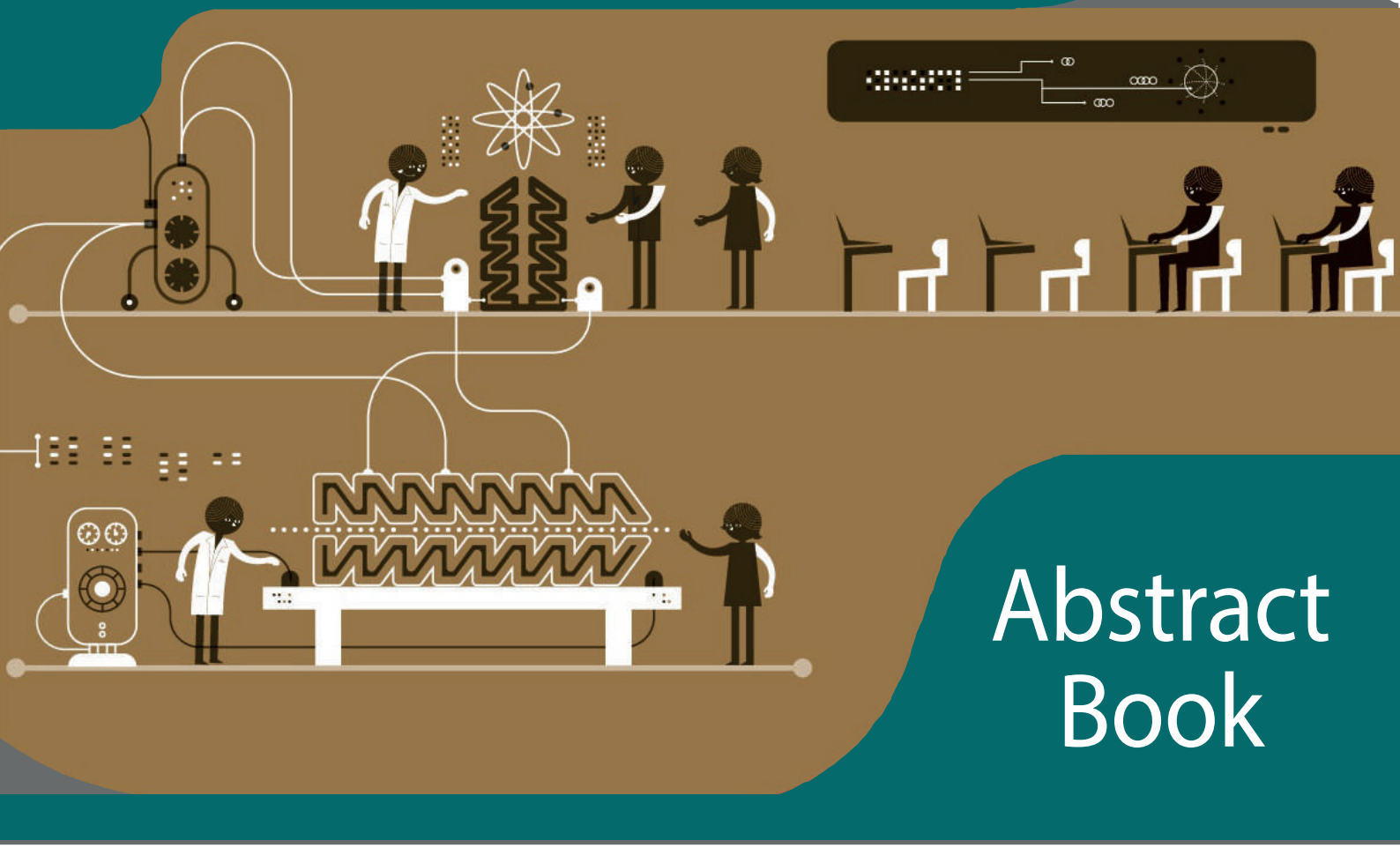

Abstract Book

NSSY 2023

Nanoscience Summer School @ Yachay 2023

April, Sunday 23rd to April Saturday 29th

Salón de la Ciudad, Santa Cruz

Galápagos-Ecuador

https://nssyconference.wixsite.com/2023

YACHAY TECH

Galápagos hub

Nanoscience Summer School 2023 @Yachay Tech International Edition

April 23rd to 29th, 2023

SCHOOL OF PHYSICAL SCIENCES AND NANOTECHNOLOGY

San Miguel de Urcuquí,
Hacienda San José s/n y Proyecto Yachay
Telephone: +593 62999500

Organizing Committee

Gema González
Sarah Briceño
Julio Chacón
Melany Aguilar Ramirez
Charlotte Berrezueta Palacios
Alexis Garzón

Support Committee

Evelyn Cifuentes
Daniela Serrano
Daniela Arellano
Angie Dávila

Scientific Committee

Duncan John Mowbray
Carlos Reinoso
Henry Pinto
Antonio Díaz
Johnny Chimborazo
David Andrade

Advisory Committee

Norman Wray
Lucia Norris

Welcome Message

On behalf of The School of Physical Sciences and Nanotechnology at Yachay Tech University in cooperation with the Governing Council of Galapagos, we invite you to join us at the third edition of the Nanoscience Summer School @ Yachay Tech 2023 (NSSY 2023).

The summer school will be held from the 23rd of April until the 29th of April 2023 at Puerto Ayora, in the Galapagos Islands, Ecuador. The NSSY 2023 will hold plenary sessions by top international scientists, invited talks from leading researchers in the field, and contributed talks chosen from the best-submitted abstracts. We will also feature a two-day poster session, which is a main focus for the program.

In this international edition of NSSY, we anticipate the participation of 120 delegates between speakers, keynotes, professor, researches and Ph.D. and Undergrad Students in an informal atmosphere where they can openly discuss, exchange ideas and results about their latest work in different topics of nanotechnology from both, theoretical and experimental points of views.

Join us at the enchanted venue of the Galapagos archipelago for the NSSY 2023 which is a must-attend for anyone interested in learning about different topics of nanotechnology, their applications, and the most recent discoveries of the field.

Welcome to the NSSY 2023 at the Galapagos islands!

Acknowledgements

The financial assistance from the sponsors and supporters is sincerely appreciated.

Horiba Scientific

The Company manufactures and sells automotive emission measurement systems, environmental measuring instruments, wide range of scientific analyzers, and medical diagnostic analyzers, and measuring equipment used in the semi-conductor industry. HORIBA also manufactures and markets peripheral measuring and analysis devices. Moreover, the Company equips such facilities as laboratories with measuring and analytical equipment for R&D, production, and other applications. The HORIBA Group of worldwide companies provides an extensive array of instruments and systems for applications ranging from automotive R&D, process and environmental monitoring, in-vitro medical diagnostics, semiconductor manufacturing and metrology, to a broad range of scientific R&D and QC measurements. Proven quality and trustworthy performance have established widespread confidence in the HORIBA Brand.

Incolor

It is a company in continuous growth and development. They currently have nationwide coverage and their satisfied customers are their best letter of introduction, count on them and benefit from their advice for your laboratory.

Mission

Provide laboratory equipment of the best quality in a way that contributes to the progress of science, education and industry in Ecuador by providing accurate technical advice and technical service that guarantees prompt attention to your requirements.

Vission

To be recognized nationally as the ideal supplier to supply specialty laboratory equipment with high quality and compliance standards.

PACIFIC CARGO LINE

Pacific Cargo Line is a leader in cargo transportation between Guayaquil and the Galapagos Islands. It offers the largest coverage in the market, covering the islands: San Cristóbal, Santa Cruz, Isabela and Floreana. In addition, it has different types of containers to transport customers' merchandise in the best possible way. This fleet of equipment is comprised of our own standard 20' and 40' containers, both for general cargo and for refrigerated cargo. As well as a range of specialized equipment such as Open Top containers and Flat Racks to carry oversized and special loads safely to their final destination.

JJ&H Cía. Ltda.

For more than 30 years, the company has been in charge of providing the best equipment for research and analysis in different areas such as Environment, Food, Geology, Materials and Industry, Forensics, Pharmaceutical, Oil, Electronics and Education.

Their services include the installation and commissioning of the equipment they provide, as well as training courses, at no additional cost to the client.

Thermofisher Scientific

Thermo Fisher Scientific supplies innovative solutions for electron microscopy and microanalysis. We provide innovative instruments combined with advanced software suites to take customers from questions to usable data by combining high-resolution imaging with physical, elemental, chemical and electrical analysis across scales and modes—through the broadest sample types.

Physical Electronics (PHI)

Physical Electronics (PHI) is a subsidiary of ULVAC-PHI, the world's leading supplier of UHV surface analysis instrumentation used for research and development of advanced materials in a number of high technology fields including: nanotechnology, microelectronics, storage media, bio-medical, and basic materials such as metals, polymers, and coatings. PHI's innovative XPS, AES, and SIMS technologies provide our customers with unique tools to solve challenging materials problems and accelerate the development of new materials and products.

Park Systems Corporation

Park Systems Corporation is the world's leading manufacturer of atomic force microscopy systems for scientific research, nanoscale engineering, semiconductor fabrication and quality assurance. Park Systems provides a full range of AFM and related products to those in the chemistry, materials, physics, life sciences, and semiconductor industries. Its customers include most of the world's largest semiconductor companies and renowned scientific research universities and national labs.


NSSY
2023


Park
SYSTEMS


JEOL

Nano
instrumentos


HOTEL
PALM
GARDEN
GALAPAGOS


Consejo de Gobierno del
Régimen Especial
de Galápagos


Proinstra S.A.
INSTRUMENTOS ANALÍTICOS
Desde 1.998


imbacorp
EXPERTOS EN COLOR DIGITAL


1835
COFFEE LAB


GAD MUNICIPAL
SANTA CRUZ
Nuestra Alcaldía


GALAPAGOS ISLANDS


COMPAÑIA DE TRANSPORTE DE CARGA PESADA
SERVPRONTGAL C.A.
Galápagos - Ecuador

Schedule

FINAL PROGRAM NSSY 2023 @ GALAPAGOS

Sunday, April 23	Monday, April 24	Tuesday, April 25	Wednesday, April 26	Thursday, April 27	Friday, April 28	Saturday, April 29
	CHARACTERIZATION OF NANOSTRUCTURES	MOLECULAR MODELING OF NANOSTRUCTURES	2D NANOMATERIALS AND HETEROSTRUCTURES	SYNTHESIS OF NANOSTRUCTURES	THEORY AND SIMULATIONS IN NANOSCIENCE	
REGISTRATION		KEY NOTE SPEAKER **Vito Despoja** 8:15 - 9:00	KEY NOTE SPEAKER **Paola Ayala** 8:15 - 9:00	KEY NOTE SPEAKER **Carlos Martínez** 8:15 - 9:00	KEY NOTE SPEAKER **Vladimiro Mujica** 8:15 - 9:00	DEPARTURE
	INSCRIPTIONS 9:00 - 11:00	INVITED SPEAKER Alicja Mikolajczyk 9:00 - 9:30	INVITED SPEAKER Mildred Quintana 9:00 - 9:30	INVITED SPEAKER Victor Guerrero 9:00 - 9:30	INVITED SPEAKER Ernesto Medina 9:00 - 9:30	
		INVITED SPEAKER Duncan Mowbray 9:30 - 10:00	INVITED SPEAKER Henrry Osorio 9:30 - 10:00	INVITED SPEAKER Lenin Ramírez 9:30 - 10:00	YOUNG RESEARCH Anthony Vizcaino 9:30 - 9:50	
		COFFEE BREAK 10:00 - 10:45				
	INAUGURATION 11:00 - 12:00	KEY NOTE SPEAKER **Carlos Sabater** 10:45 - 11:30	ORAL CONTRIBUTION Igor Carvhalo 10:45 - 11:15	INVITED SPEAKER Raúl Dávalos 10:45 - 11:15	YOUNG RESEARCH Charlotte Berrezueta 10:45 - 11:05	
			YOUNG RESEARCH Verónica Quilumba 11:15 - 11:35	ORAL CONTRIBUTION Hilda Zavaleta 11:15 - 11:45	YOUNG RESEARCH Joselyn Benalcazar 11:05 - 11:25	
			YOUNG RESEARCH Adriana Vázquez 11:35 - 11:55	ORAL CONTRIBUTION Igor Carvhalo 11:45 - 12-15	CLOSING REMARKS 11:25 - 11:55	
	PLENARY TALK **Vincent Meunier** 14:00 - 15:00		CONFERENCE TOUR 13:00 - 19:00			
	INVITED SPEAKER Patricio Espinoza 15:00 - 15:30	POSTER SESSION I 15:00 - 17:45		POSTER SESSION II 15:00 - 17:45		
	INVITED SPEAKER Carla Bittencourt 15:30 - 16h00					
	COFFEE BREAK 16:00 - 16:45					
	INVITED SPEAKER Jorge Serrano 16:45 - 17:15					
	ORAL CONTRIBUTION Carlos Reinoso 17:15 - 17:45					
WELCOME RECEPTION	ORAL CONTRIBUTION Andrey Mereshkenko 17:45 - 18:15	PLENARY TALK **Eduard Llobet** 18:00 - 19:00		KEY NOTE SPEAKER **Denis Kochan** 18:00 - 18:45		
	YOUNG RESEARCH Jonathan Escorza 18:15 - 18:35					
	ORAL CONTRIBUTION Johnny Chimborazo 18:35 - 19:05					
	DINNER 19:05 - 21:00	DINNER 19:00 - 21:00	DINNER 19:00 - 21:00	DINNER 19:00 - 21:00	DINNER 19:00 - 21:00	

Acta Microscopica Vol. 32, Supp. 1, 2023, pp. xx
PROCEEDINGS NSSY 2023- Galapagos 23th-29th April 2023

MONDAY

Characterization of Nanostructures

Acta Microscopica Vol. 32, Supp. 1, 2023, pp. xx
PROCEEDINGS NSSY 2023- Galapagos 23th-29th April 2023

RAMAN SPECTROSCOPY: A TUTORIAL

Vincent Meunier (1)

(1) Engineering Science and Mechanics Department, The University of Pennsylvania, State College, PA, USA
vincent.meunier@psu.edu

Raman spectroscopy is a spectroscopic technique used to measure the vibrational modes of materials. Raman spectroscopy is a popular technique used in chemistry and material science and has proven one of the key techniques in the development of nanoscience and nanotechnology. This technique relies on inelastic scattering of photons. The photons (e.g., monochromatic light from a laser) interact with the electronic properties of a material and, during the process, can excite phonon (i.e., vibrational) modes. Due to energy conservation requirements, the scattered light's energy is shifted by an energy that corresponds to the existing phonon mode, and which can then be determined. For this reason, Raman spectroscopy can be used to examine the intrinsic fingerprints of materials and molecules. As a non-destructive and fast technique, Raman has repeatedly proven effective for the quantitative determination of their properties. The interpretation of many experimental features requires a dedicated modeling effort based on first-principles methodologies. Fortunately, at the same time as experimental characterization and sample preparation techniques have evolved to new heights, theoretical schemes are now combined with unprecedented computational resources to provide tools akin to a *virtual microscope* to enable the translation of experimental data into a fundamental understanding of intrinsic properties of the investigated samples.

Here, I will summarize the fundamental features of Raman spectroscopy, focusing on nanomaterials as test subjects. Using a semi-classical framework, I will provide a pedagogical step-by-step introduction to Raman spectroscopy with the objective of teaching students how to read Raman spectra and find ways to interpret them. I will introduce concepts such as Rayleigh, Stokes, and anti-Stokes mechanism and show the importance of light polarization in the determination of the Raman spectrum. I will explain what Raman practitioners mean about the concept of "Raman active modes". Finally, if time permits, I will also introduce the outline of a full quantum mechanical treatment of resonant Raman spectroscopy. In the second part of my talk, I will describe how Raman can be used to obtain a determination of the structural details of defective [1] and finite-size nanoribbons [2]. Furthermore, I will discuss the importance of low-frequency modes in the study of layer-layer interactions in TMDs and phosphorene, how relative twisting angles can be determined by monitoring relative shifts in Raman active mode in $MoSe_2$, and how Raman can be employed to understand in-plane anisotropy in phosphorene. Finally, I will show how defect concentration (notably, S vacancy density) can be determined by the sole knowledge of the shift in major vibration modes of MoS_2 subjected to electron irradiation [3].

REFERENCES

[1] O Gröning, et al, *Engineering of robust topological quantum phases in graphene nanoribbons,* Nature 560 (7717), 209-213 (2018)
[2] J Overbeck et al, *A universal length-dependent vibrational mode in graphene nanoribbons,* ACS nano 13 (11), 13083-13091 (2019)
[3] W. Parkin et al. *Raman shifts and in situ TEM electrical degradation of electron-irradiated monolayer MoS_2,* submitted (2016)

ACKNOWLEDGMENTS

Vincent Meunier thanks support from the Focus Center at Rensselaer Polytechnic Institute, a NYS Department of Economic Development award (No. A21-0125-002 and RPI designation A50634.2326) and from the Pennsylvania State University.

FIGURES

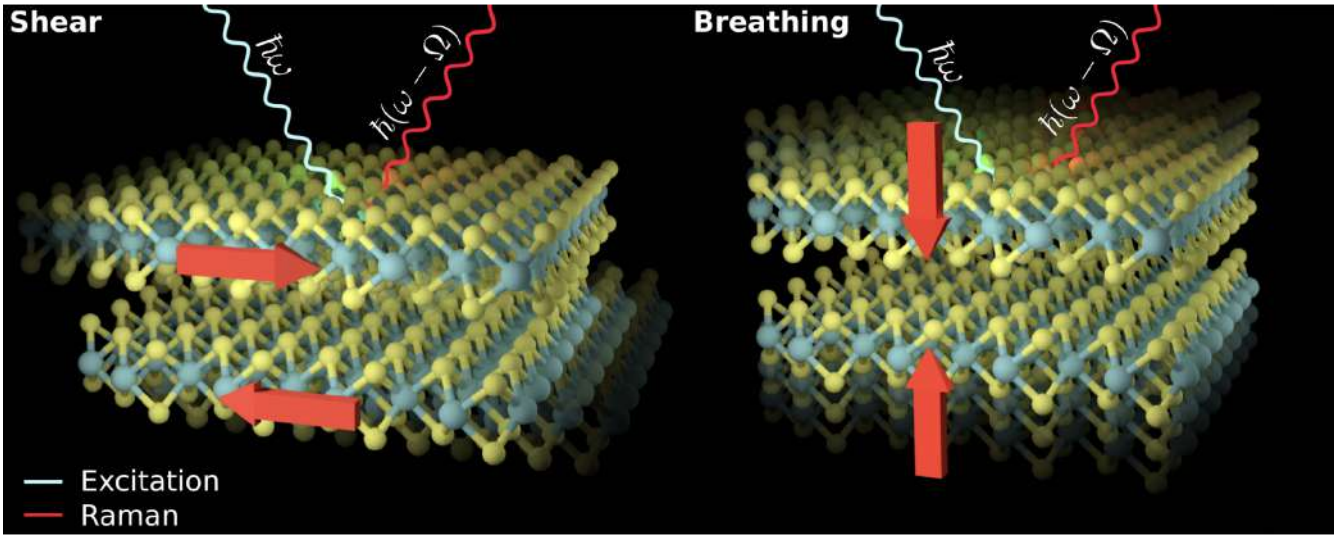

Figure 1. Schematic representation of the interlayer Raman processes taking place in bilayered MoS_2 material.

Acta Microscopica Vol. 32, Supp. 1, 2023, pp. xx
PROCEEDINGS NSSY 2023- Galapagos 23th-29th April 2023

TiO_2-MODIFIED BORON-DOPED DIAMOND PHOTOANODES FOR EFFICIENT PHARMACEUTICAL, PESTICIDE AND MICROPLASTICS PHOTOELECTROCATALYTIC DEGRADATION

Patricio J. Espinoza-Montero[1], Paulina Alulema-Pullupaxi[1,2], Carol Sigcha-Pallo[1,2], Wendy Quilumbaquin[1], G. Xavier Castillo-Cabrera[1]

Pontificia Universidad Católica del Ecuador, Escuela de Ciencias Químicas, Quito 170525, Ecuador. pespinoza646@puce.edu.ec. (2) Escuela Politécnica Nacional, Departamento de Ingeniería Civil y Ambiental, Quito-Ecuador
pespinoza646@puce.edu.ec

Pollution of natural effluents caused by population growth, industrial development and the expansion of the agricultural frontier is a serious problem that has received scarce attention. Recalcitrant and contaminants of emerging concern (CECs) (i.e. pharmaceuticals, agrochemicals, microplastics, detergents, dyes, phenolic derivatives, etc.) are both an environmental and a health problem, mainly due to its toxicity and possible hazardous effects on living organisms, including humans. Conventional wastewater treatments have not been able to efficiently remove contaminants from water; nevertheless, electrochemical advanced oxidation processes (EAOPs) can address this environmental issue. One of the most popular EAOPs technologies today is photoelectrocatalysis (PEC). The PEC consists of: i) light absorption on the photocatalyst-semiconductor thin film supported on a conductive substrate (photoelectrode) (light energy > photocatalyst band-gap), generating electron-hole (e^-–h^+) charge carriers; ii) extraction of the electrons from the conduction band (CB) of the photoanode to the external circuit, applying an external bias potential; iii) the occurrence of the surface redox reactions (h^+ generate $^{\bullet}OH$), Figure 1. The hydroxyl radical ($^{\bullet}OH$) is the second strongest oxidant in nature after fluorine, responsible for the degradation/mineralization of organic pollutants in aqueous media. [1]. In this regard, the construction of boron-doped diamond photoanodes modified with titanium dioxide (BDD/TiO_2) is presented by two methods for the fabrication of thin-film photoelectrodes, one by in situ synthesis of the photocatalyst (sol-gel spin coating) and the other by surface modification of the commercial photocatalyst (electrophoresis). Their surface, electrochemical and photoelectrochemical characterisation is presented. In addition, the results of the application of BDD/TiO_2 photoanodes in the efficient photoelectrocatalytic degradation of glyphosate [2] and diclofenac [3], as well as the deterioration/fragmentation of microparticulated high-density polyethylene (HDPE) in synthetic water samples are shown. An increase in the degradation rate of both paracetamol and diclofenac by FEC is highlighted as a result, compared to the results obtained by electrochemical advanced oxidation (EAO). In the case of the treatment of microplastics by FEC, a greater effectiveness is achieved in the deterioration of HDPE microspheres compared to AEO. In this way, it is evidenced that the modification of the BDD electrode with TiO_2 favors the injection of charge carriers, and in this fashion the transfer at the photoelectrode-solution interface is improved. In addition, it is demonstrated that the electrodes obtained by both techniques of thin film deposition present a high stability during the degradation cycles to which they were subjected.

REFERENCES

[1] G. X. Castillo-Cabrera, P. J. Espinoza-Montero, and P. Alulema-Pullupaxi, “Bismuth Oxyhalide-Based Materials (BiOX : X = Cl , Br , I) and Their Application in Photoelectrocatalytic Degradation of Organic Pollutants in Water : A Review,” *Front. Chem.*, vol. 10, pp. 1–19, 2022.
[2] P. Alulema-Pullupaxi *et al.*, “Photoelectrocatalytic degradation of glyphosate on titanium dioxide synthesized by sol-gel/spin-coating on boron doped diamond (TiO_2/BDD) as a photoanode,” *Chemosphere*, vol. 278, 2021.
[3] C. Sigcha-Pallo *et al.*, “Photoelectrocatalytic degradation of diclofenac with a boron-doped diamond electrode modified with titanium dioxide as a photoanode,” *Environ. Res.*, vol. 212, p. 113362, Sep. 2022.

ACKNOWLEDGMENTS

The authors are grateful to the Pontifical Catholic University of Ecuador for financial support for the project "Preparation of boron-doped diamond (BDD) photoelectrodes modified with bismuth semiconductors and their application in photoelectrocatalysis". Code: 030-UIO-2023.

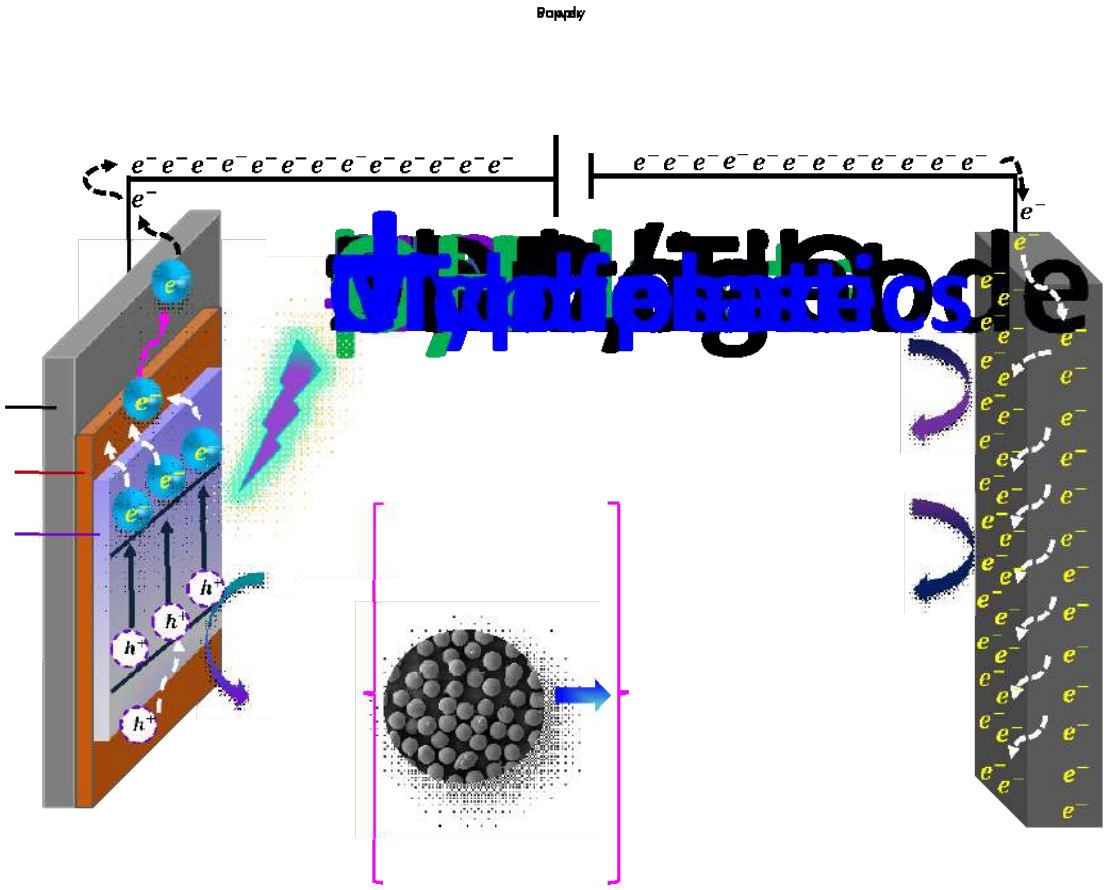

Figure 1. Photoelectrocatalytic mechanism based on a boron-doped diamond photoanode modified with titanium dioxide (BDD/TiO_2).

Acta Microscopica Vol. 32, Supp. 1, 2023, pp. xx
PROCEEDINGS NSSY 2023- Galapagos 23th-29th April 2023

Acta Microscopica Vol. 32, Supp. 1, 2023, pp. xx
PROCEEDINGS NSSY 2023- Galapagos 23th-29th April 2023

NEAR-ATMOSPHERIC PRESSURE X-RAY PHOTOELECTRON SPECTROSCOPY APPLIED TO STUDY THE SENSING DETECTION MECHANISM OF TRANSITION METAL DICHALCOGENIDES

Aanchal Alagh (1), Fatima Ezahra Annanouch (1), Eduard Llobet (1) and Carla Bittencourt (2).

(1) Department of Electrical Electronic Engineering and Automation, Universitat Rovira i Virgili, Tarragona, Spain.
(2)Plasma-Surface Interaction Chemistry, Chemistry Department, University of Mons, Mons, Belgium.
carla.bittencourt@umons.ac.be

The interface between gasses and solids governs many processes, such as energy generation and heterogeneous catalysis, that are key for the development of new technologies. Many surface-sensitive spectroscopies and microscopies can be used to study vapor/solid interfaces; among them, X-ray photoelectron spectroscopy (XPS) is one of the most versatile. It is highly surface sensitive due to the photoelectrons' short mean free path, providing quantitative information about the surface's elemental composition and chemical specificity (e.g., oxidation state).

Despite the usefulness of XPS measurements in ultra-high vacuum (UHV) for determining the chemical composition of active layers, UHV studies may not capture changes in surface chemical composition in the presence of an analyte gas. Such information is, however, vital for understanding how a device based on gas-surface interaction works. Since photoelectrons are strongly scattered by gas molecules, the use of XPS at elevated pressures was ruled out until very recently. For instance, the inelastic mean free path of an electron with 100 eV kinetic energy with 1mbar water vapor is about 1mm, much shorter than the typical working distance between the sample surface and the entrance to the electrostatic lens of an electron analyzer, which is a few centimeters.

However, advances in vacuum technology have led to the development of a variety of photoelectron spectrometers using differential vacuum pumping that can now operate at up to approximately 130 mbar [1,2]. This technique is known as near ambient pressure (NAP) or high pressure (HP) XPS to distinguish it from traditional vacuum-based XPS [3]. The unique combination of surface sensitivity, element specificity, and elevated pressure operation makes NAP-XPS ideal for an ‘in-situ/in-operando’ investigation of the chemical composition and mechanisms of surface processes central to the operation of gas sensing.

Research on graphene has been based on its use as a replacement for silicon in electronics. However, it is now unlikely to happen. Instead, novel applications have emerged. Bearing in mind the history of the development of graphene research, for nanostructured transition metal dichalcogenides to have an impact, new technologies must be based on their unique properties and not on the possibility of replacing materials used in present technologies.

Continuous and reliable detection of different gasses is essential in industrial process monitoring, vehicle emission control, indoor and outdoor air quality safety, and environmental protection. Traditionally, metal oxide semiconductors have been commonly utilized in these applications as sensing materials. While these sensors and their arrays offer fair discrimination and even quantification of analytes, their operation is only possible at high temperatures, which requires considerable power sourcing. Nowadays, with the spread of internet-of-things and wireless networks that involve complex sensing systems with a small but large number of devices, power consumption becomes a significant factor. Novel materials that would allow for the low-temperature operation could alleviate power-related challenges and contribute to better and more robust

sensor networks. In this context, 2D layered transition metal dichalcogenides (TMDs) have recently been found very attractive for chemo-resistive sensors. Recent studies of WS2 and MoS2 as gas sensor active layers indicate substantial response at low operating temperatures with particular selectivity to certain gasses such as NO2, H2S, and NH3. The lowered operation temperature of transition metal chalcogenide-based sensors, in reference to metal oxides, is due to their typically lower bandgap and better conductivity. Furthermore, similarly to semiconducting metal oxide sensors, the gas selectivity of TMDs is often associated with their surface's affinity for adsorbing different analytes and related surface charging/polarization effects. In addition, it has been identified that apart from surface charging/polarization, reversible doping of the chalcogenide lattice with heteroatoms can significantly contribute to sensing. Although very valuable, most of the reports are based on extra-situ measurements. Although many works discuss sensing mechanisms of TMDs materials under dry conditions or in the presence of ambient moisture, these are speculative since few operando spectroscopic studies are available for elucidating these.

We will report on the use of NAP-XPS to study the sensing of WS2 and Cu2O-WS2 nanostructured films. The films were prepared by CVD. The survey and high-resolution XPS spectra of W, O, and C, and S were measured before and during exposure at different (gas pressure conditions) at the two operating temperatures (RT and 150oC). The samples were heated from underneath using an IR-laser. The sample´s resistance was measured when collecting the XPS data (in operando analysis). These experiments allow correlating the changes at the sample surface with the sensing properties of WS2 and Cu-WS2 nanomaterials: which factors (oxygen species, tungsten oxidation state, adsorbed intermediate species) most influence the sensing properties. In-situ analysis of the interaction of CO with the WS2:Cu2O surface: the spectrum recorded during interaction suggests a change in the surface potential supported by the observation of a simultaneous change in the conductivity of the sample (in operando). The relative intensity of the two components in the O 1s peak changed due to the CO interaction indicating the participation of the tungsten oxide in the WS2:Cu2O sensing at low temperatures.

To better understand the effect of materials morphology and metal oxide loading on the gas sensing mechanism as well as improve sensing properties, we characterize the surface composition and electronic structure of the nanomaterials under real conditions. That is at the sensor operating temperature, during the exposure to oxygen, and then during the exposure to CO and H2. The role of having or lacking adsorbed water at the surface by exposing WS2 to moisture was evaluated. By identifying the intermediate species adsorbed together with the measurement of electrical conductance, we expect to unveil the morphology-performance correlation in the detection of CO and H2. NAP-XPS is a unique technology capable of conducting this type of analysis under realistic operating conditions.

REFERENCES

[1] Ueda K. et al. ACS Catal. (2018) (8) (12) (11663).
[2] Starr D.E. et al. Chem. Soc. Rev. (2013) (42) (5833).
[3] Junker B. et al. J. Phys. D: Appl. Phys. (2022) (55) (064002).

ACKNOWLEDGMENTS

C. B. is a Research Associate of the National Funds for Scientific Research (FRS-FNRS, Belgium; E. L. is supported by the Catalan Institute for advanced studies (ICREA)) via the 2018 Edition of the ICREA.

Acta Microscopica Vol. 32, Supp. 1, 2023, pp. xx
PROCEEDINGS NSSY 2023- Galapagos 23th-29th April 2023

CONTROLLING DOPING PROFILES OF SILICON NANOWIRES FOR QUANTUM COMPUTING AND PHOTOVOLTAICS USING MICRO-RAMAN SPECTROSCOPY

Jorge Serrano (1), Vanessa Giselle Hinojosa Chasiquiza (1), Irene Mediavilla Martínez (1), Juan Jiménez (1), David Bricio (2), Francesc Pérez-Murano (2), Jordi Llobet (2), Jordi Antonja (3), Joan Bausells (2), Franck Bassani (4), Bassem Salem (4), Thierry Baron (4).

(1) Grupo OPTRONLAB, Dep. de Física de Materia Condensada, Cristalografía y Mineralogía, Universidad de Valladolid, Edificio LUCIA, Paseo de Belén 19, 47011 Valladolid, Spain. (2) Instituto de Microelectrónica de Barcelona IMB-CNM, CSIC, 08193 Bellaterra, Barcelona, Spain. (3) CELLS-ALBA Synchrotron, Carrer de la Llum 2-26, Cerdanyola del Vallès 08290, Spain. (4) LTM-CNRS, CEA-LETI, 17 rue des Martyrs, 38054 Grenoble Cedex, France.
jorge.serrano@uva.es

Silicon technology has been the cornerstone for the advance of the current age of information since the inception of the first transistor, due to an exponential development of microelectronics and chip miniaturization. Based on this success, some of the emerging technologies in photovoltaics and quantum computing are being developed using silicon nanowires as a fundamental building block. In the case of photovoltaics, p-n axial and core-shell junctions in Si nanowires allow the integration of silicon technology with other materials and thus a potential larger solar cell efficiency [1]. In quantum computing, silicon nanowires serve as one of the semiconducting platforms for qubit development by controlling the electron spin levels using a tailored selected doping and voltage in gates that split the nanowire into different quantum dots [2]. In both scenarios it is of paramount importance to control several key parameters, among them the dopant concentration in the nanowire, the stress, and the concentration of defects. They can all affect the operation of the corresponding device and result in critical failure or lack of reliability. Accessing these parameters with nanoscale resolution has been a challenge for spectroscopic techniques due to the diffraction limit of currently widespread optical spectroscopy. We present here a characterization using micro-Raman imaging and tip-enhanced Raman spectroscopy (TERS) that shows the potential of these techniques to determine the doping profile of silicon nanowires in both p-n junctions and silicon nanostructures for qubits, and to distinguish doping effects from others such as the presence of strain, crystal grains, and defects. High dopant concentrations lead to Fano asymmetric line shape of the Raman spectrum of silicon with an asymmetry parameter proportional to the dopant concentration and character – p- or n-type doping [3]. Confinement of the electric field due to the nanoscale diameter of the nanowires results in an enhancement of the Raman signal that yields higher resolution than that expected without this antenna effect. This enhancement allows us to employ micro-Raman spectroscopy successfully to distinguish several of the above mentioned effects in nanostructures. In the case of p-n axial junctions in silicon nanowires, we observe an asymmetry with higher spectral weight in the low and high energy side for p-type and n-type doping, respectively, being the effect more pronounced in the case of p-type doping. This effect is more significant for doping concentrations above 10^{17} cm^{-3}. In the case of nanostructured silicon for qubits we observe residual strain and crystallite grain boundaries close to the nanowire, tentatively attributed to the presence of We analyze the Raman spectra employing several asymmetric functions and compare the results obtained in nanowires with those reported in the literature and achieved in bulk silicon as a function of doping. Finally, we employ TERS to reach nanoscale spatial resolution and compare the accuracy and limitations of micro-Raman in the determination of the doping profile.

REFERENCES

[1] Li, G., Kwok, HS. (2018). *Silicon Nanowire Solar Cells*. In: Ikhmayies, S. (eds) Advances in Silicon Solar Cells. Springer, Cham, pp. 269.
[2] Maurand R. et al. *Nat. Commun.* (2016) (7) (13575).
[3] U. Fano, *Physical Review* (1961) (124) (1866).

ACKNOWLEDGMENTS

J. Serrano, V.G. Hinojosa Chasiquiza, I. Mediavilla-Martínez, and J. Jiménez acknowledge financial support by AEI grants PID2021-126046OB-C22 and TED2021-130786B-I00 (Spain). D. Bricio, J. Llobet, J. Antonja, F. Pérez-Murano, and J. Bausells acknowledge financial support by AEI grant PID2021-126046OB-C21 (Spain).

FIGURES

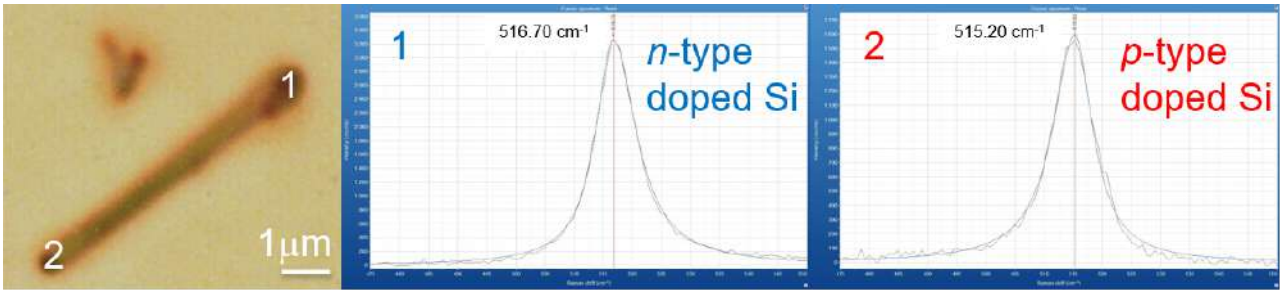

Figure 1. (left) Optical microscopy image of a *p-n* axial junction silicon nanowire (NW). The numbers 1 and 2 denote the *n-* and *p*-type sides of the junction. (center) Typical micro-Raman spectrum of the *n*-type side of the *p-n* axial junction Si NW fitted with a Fano lineshape. Note the asymmetric broadening towards the high energy side. (right) Typical micro-Raman spectrum of the *p*-type side of the *p-n* axial junction Si NW fitted with a Fano lineshape. Note the asymmetric broadening towards the low energy side.

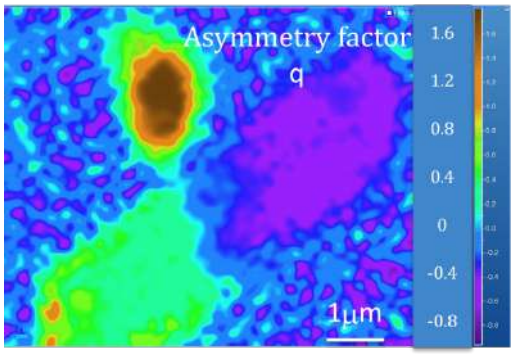

Figure 2. Color map of asymmetry factor *q* from a modified Fano function [3] fit of the micro-Raman spectra at the *p-n* axial junction Si NW shown in Fig. 1. Taken with an excitation laser of 532 nm wavelength, 4.5 mw power and 0.2 s acquisition time. Note the positive and negative values for the asymmetry factor corresponding to *p-* and *n*-type doping edges, respectively.

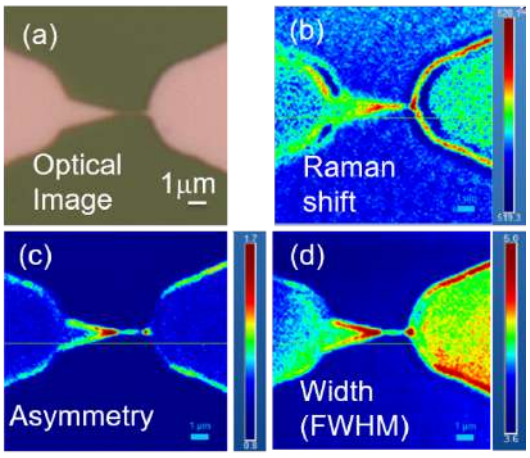

Figure 3. (a) Optical microscopy image of the contacts and Si NW region of a Silicon-on-insulator bottom-up structure for development of Si qubits. Color maps of (b) Raman shift, (c) asymmetry parameter, and (d) full width at half maximum (FWHM) of asymmetric Lorentzian fit to the micro-Raman map of spectra taken with constant step of 0.1 microns and similar wavelength and power than that of Figs. 1 and 2. The small but significant changes in the Raman shift indicate strain induced at the contacts and NW region due to the lithography and etching processing, whereas those of the asymmetric parameter display a combination of the growth of the grain boundaries at the Si NW and the increased doping at that region.

Acta Microscopica Vol. 32, Supp. 1, 2023, pp. xx
PROCEEDINGS NSSY 2023- Galapagos 23th-29th April 2023

FABRICATION OF ELECTRODES WITH MWCNTS-FUNCTIONALIZED PVDF POLYMERIC MEMBRANES TO BE APPLIED ON MICROBIAL FUEL CELLS.

León Ocaña (1), Orlando Salguero (1), Jonathan Escorza (1), Yolanda Angulo (2), Carlos Reinoso (1).

(1) School of Physical Sciences and Nanotechnology, Universidad de Investigación de Tecnología Experimental Yachay, Urcuquí-Ecuador.
(2) Center for Nanoscience and Nanotechnology, Universidad de las Fuerzas Armadas, Sangolquí-Ecuador.
creinoso@yachaytech.edu.ec

Energy consumption has been growing significantly over the past few decades, with an increasing demand for power to fuel a range of activities, including industrial processes, transportation, and household electricity use. This trend is expected to continue in the future, highlighting the importance of finding alternative, sustainable energy sources. One potential solution is the use of microbial fuel cells (MFCs), which can generate electricity through the decomposition of biomass with the help of functionalized electrodes. These MFCs have several advantages over traditional power generation methods, including a lower environmental impact and the ability to utilize waste materials as fuel. However, one of the challenges in using MFCs is developing efficient and cost-effective electrodes [1]. To address this issue, our research aimed to design a drop angle analysis system to produce conductive coatings using polyvinylidene fluoride (PVDF) membranes dissolved in dimethylacetamide (DMA) and multiwalled carbon nanotubes (MWCNTs) dispersed in varying concentrations. Metal meshes were then used to support these coatings and create the electrodes. To assess the performance of the resulting electrodes, we employed several characterization techniques, including electrochemical impedance spectroscopy (EIS) and cyclic voltammetry (CV) and the SEM images make evident a porosity surface as is seen in Figure 1. These measurements enabled us to optimize the number of layers and the concentration of MWCNTs to achieve the best results in terms of voltage generation. Our results showed that our optimized electrodes were able to generate approximately 100 millivolts of voltage, demonstrating their potential for use in MFCs. Moreover, our approach offers a low-cost alternative that could be particularly valuable for developing countries that lack the resources to invest in more expensive technologies. In addition to the development of MFC electrodes, our research highlights the importance of nanotechnology in advancing sustainable energy solutions. Nanomaterials, such as MWCNTs, have unique properties that make them suitable for a range of energy applications [2]. For example, their high surface area to volume ratio and excellent electrical conductivity makes them ideal for use in energy storage devices and solar cells, also related with the porosity. Nanotechnology has also enabled the development of new materials with improved properties for use in energy conversion and storage. For instance, researchers have designed new catalysts that can improve the efficiency of hydrogen fuel cells, which convert hydrogen into electrical energy. Nanomaterials have also been used to improve the performance of lithium-ion batteries, which are widely used in portable electronics and electric vehicles. In conclusion, the need for sustainable energy solutions is becoming increasingly urgent in the face of rising energy demands and the ongoing climate crisis. Our research demonstrates the potential of MFCs as a renewable energy source, and the importance of developing cost-effective electrodes for this technology. Moreover, our work highlights the significant role that nanotechnology plays in developing sustainable energy solutions, and the potential for further advances in this field to help address the world's energy needs. Cyclic Voltammetry (CV) and Potentiostatic Electrochemical Impedance Spectroscopy (PEIS) are analytical techniques used to investigate the conductive behavior of materials. In this study, the conductive properties of two membranes with varying concentrations of Multiwalled Carbon Nanotubes (MWCNTs) were analyzed using these techniques [3]. The results of the CV analysis revealed the conductivity of the membranes as is seen in Figure 2. The slope of the lines on the graph indicated the conductivity of each membrane, with steeper slopes representing higher conductivities. On the other hand, the PEIS analysis showed the impedance of the membranes. A higher concentration of MWCNTs resulted in lower impedance and, therefore, higher conductivity. These findings have important implications for the design and

optimization of Microbial Fuel Cells (MFCs), which rely on the conductive properties of electrodes to harvest electrons from the decomposition of biomass. By using membranes with high conductivity, MFCs can generate higher voltages and be more effective in converting organic matter into electrical energy.

REFERENCES

[1] Kaur R, Marwaha A, Chhabra VA, Kim KH, Tripathi SK. Recent developments on functional nanomaterial-based electrodes for microbial fuel cells. Renewable and Sustainable Energy Reviews. 2020 Mar 1;119:109551.

[2] Hinds, B. J. (2004). Aligned Multiwalled Carbon Nanotube Membranes. Science, 303(5654), 62–65. doi:10.1126/science.1092048

[3] Streeter I, Wildgoose GG, Shao L, Compton RG. Cyclic voltammetry on electrode surfaces covered with porous layers: an analysis of electron transfer kinetics at single-walled carbon nanotube modified electrodes. Sensors and Actuators B: Chemical. 2008 Aug 12;133(2):462-6.

ACKNOWLEDGMENTS

YA acknowledge to the grant PIC001 2020 from ESPE. OS, LO, CA acknowledge the School of Physical Sciences and its laboratories for the use of the equipment.

FIGURES

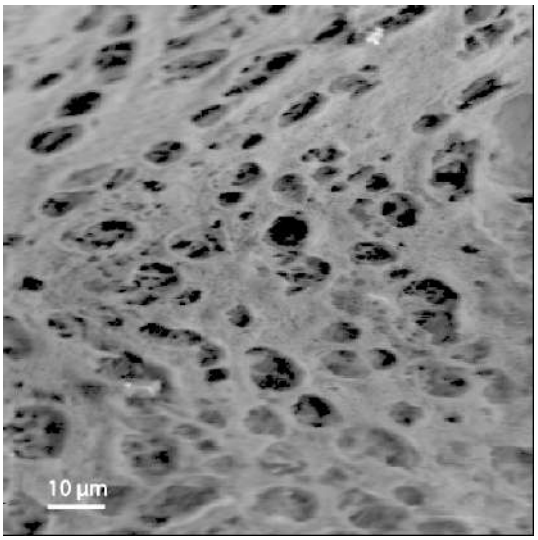

Figure 1. SEM of Electrode surface, the porosity facilitates the interaction between microbials, and the functionalized electrode.

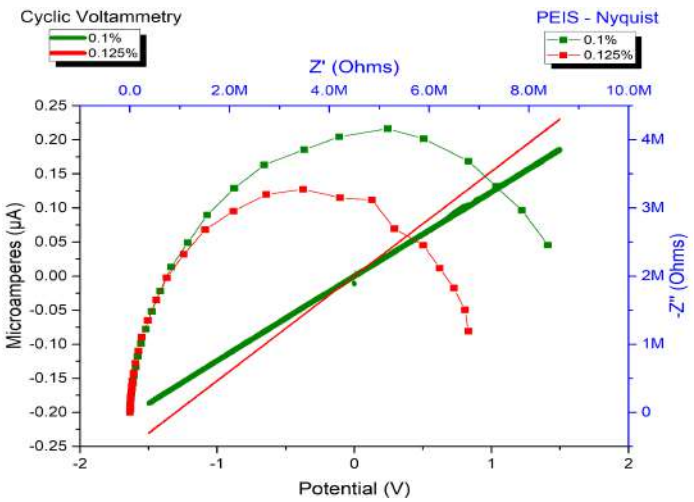

Figure 2. The slope of the lines on the Cyclic Voltammetry (CV) indicated the conductivity. Higher concentration of MWCNTs resulted in lower impedance and, therefore, higher conductivity in the (PEIS) measurement.

Acta Microscopica Vol. 32, Supp. 1, 2023, pp. xx
PROCEEDINGS NSSY 2023- Galapagos 23th-29th April 2023

$NaGdF_4:Eu^{3+}$ NANOMATERIALS AS MAGNETIC AND OPTICAL PROBES OF BIOLOGICAL SYSTEMS

Andrey S. Mereshchenko (1), Anna A. Betina (1), Tatyana S. Bulatova (1), Bulat S. Akhmadeev (2)

(1) Institute of Chemistry, Saint-Petersburg State University, 7/9 Universitetskaya emb., 199034 St. Petersburg, Russia
(2) A. E. Arbuzov Institute of Organic and Physical Chemistry, Kazan Scientific Center, Russian Academy of Sciences, Arbuzov str., 8, 420088, Kazan, Russia.
a.mereshchenko@spbu.ru

Inorganic nanomaterials containing lanthanide ions are widely studied due to their optical and magnetic properties and broad application within such areas as the design of luminescent thermometers, photocatalysts, solid-state lasers, and solar cells, the development of sensors of biologically important substances, drugs for thermal therapy of tumors and MRI contrast agents, and so on. Such compounds allow making multifunctional materials through a combination of optical, magnetic, radioactive, and other properties, which make them attractive and promising materials for theranostics [1]. These properties make it possible to design multimodal materials for molecular imaging and non-invasive optical diagnostics of tissues of living organisms in vivo using magnetic resonance imaging (MRI), as well as materials for the detection and targeted treatment of cancer cells at early stages of the disease. In this work, we present the results of a study of $NaGdF_4$: Eu^{3+} nanocrystalline materials, which combine luminescent and paramagnetic properties. $NaGd_{1-x}Eu_xF_4$ compounds with different contents of europium and gadolinium (x = 0 - 1) were obtained by hydrothermal synthesis using citric acid as a stabilizing agent [2,3]. Rare earth chlorides taken in stoichiometric amounts (total amount of rare earth chlorides was 0.75 mmol) with 3 mmol of citric acid were dissolved in distilled water to obtain 5 mL solution in total. Then, 2.5 mL of an aqueous solution containing 9 mmol of NaOH was added to the flask of the previous solution. After vigorous stirring for 30 min, 8 mL of aqueous solution containing 11 mmol of NaOH and 11 mmol of NH_4F was added into the above solution. The solution was maintained after vigorous stirring for 30 min at room temperature before being transferred to a Teflon-lined autoclave with an internal volume of 20 mL and heated for 17h at the temperature of 180 °C. After that, the precipitate was separated from the reaction mixture by centrifugation, washed with ethanol and deionized water, and either stabilized by the surfactant or dried at 60 °C for 24 h. We found that all synthesized compounds are solid solutions and have hexagonal β- $NaYF_4$ crystalline phase. Analysis of powder diffraction patterns showed that the substitution of gadolinium ions for larger europium ions leads to an increase in the unit cell parameters and its volume. The linear dependence of the unit cell volume on the concentration of europium ions shows that Vegard's law is obeyed for this series of solid solutions. Scanning electron microscopy showed that the samples consist of particles that have a shape of hexagonal prisms, the average particle size lies in the range of 35–45 nm, and the particle size is practically independent of the composition. The luminescence spectra of the synthesized materials were measured upon excitation at the wavelength of 393 nm into the $^5L_6$ electronic state. The emission spectra consist of narrow lines corresponding to f-f transitions from excited $^5D_0$ to lower energy levels: $^5D_0$–$7F_0$ (582 nm), $^5D_0$–$^7F_1$ (589 nm), $^5D_0$–$^7F_2$ (614 nm), $^5D_0$–$^7F_3$ (649 nm) and $^5D_0$–$^7F_4$ (688 and 694 nm). The radiative transitions $^5D_0$–$^7F_1$ and $^5D_0$–$^7F_2$ are characterized by the highest intensities. The spectra also contain low-intensity transitions from the $^5D_1$ and $^5D_2$ levels to different ^7F_J levels: $^5D_2$–$^7F_2$ (486 nm), $^5D_2$–$^7F_3$ (508 nm), $^5D_1$–$^7F_1$ (524 and 534 nm), nm). The highest luminescence intensity was observed for the $NaGd_{0.7}Eu_{0.3}F_4$ compound; concentration quenching occurs at the higher content of europium ions. $NaGd_{0.7}Eu_{0.3}F_4$ nanoparticles are paramagnetic, the magnetic susceptibility is $7.2 \cdot 10^{-5}$ emu g^{-1} Oe^{-1}, which corresponds to the expected for $NaGdF_4$: Eu^{3+} solid solutions. In order to further use the obtained materials as polymodal bioimaging agents, $NaGd_{0.7}Eu_{0.3}F_4$ particles of about 40 nm in size were stabilized in an aqueous solution using various surfactants: polyvinylpyrrolidone (PVP), sodium dodecyl sulfate (SDS) and cetrimonium bromide (CTAB). It has been shown that CTAB-modified particles are stable in an aqueous solution for at least 48 hours, whereas unmodified particles and particles covered by SDS and PVP aggregate. According to luminescent confocal microscopy, $NaGd_{0.7}Eu_{0.3}F_4$@CTAB and $NaGd_{0.7}Eu_{0.3}F_4$@SDS samples are able to penetrate into HeLa cells showing notable red emission upon 390-nm excitation. The transverse magnetic relaxivity r_2 of the $NaGd_{0.7}Eu_{0.3}F_4$@CTAB sample is 161±7 $s^{-1}mM^{-1}$, which is comparable to commercial contrast agents for

magnetic resonance imaging. The evaluation of the cytotoxicity of colloidal solutions of $NaGd_{0.7}Eu_{0.3}F_4$, $NaGd_{0.7}Eu_{0.3}F_4$@CTAB, and $NaGd_{0.7}Eu_{0.3}F_4$@SDS particles was carried out on HeLa, HEP2-G, and HEK-293 cell lines. The obtained IC50 cell survival values are 15 mg/l for HeLa and more than 25 mg/l for HEP2-G and HEK-293, indicating a low cytotoxicity of these materials. Also, all colloidal solutions demonstrate good hemocompatibility. The data obtained indicate the possible application of surfactant-stabilized $NaGd_{0.7}Eu_{0.3}F_4$ nanoparticles as contrasts for MRI and dyes for luminescence microscopy in living organisms.

REFERENCES

[1] Dong H. et al. *Chem. Rev.* (2015) (115) (10725)
[2] Kolesnikov, I.E. et al. *New J. Chem.* (2021) (45) (10599)
[3] Bogachev N.A. et al. *Nanomaterials* (2022) (12) (2972)

ACKNOWLEDGMENTS

This research was funded by Fellowship of President of Russia MD-1191.2022.1.3. The measurements were performed at the Research Park of Saint-Petersburg State University (''Magnetic Resonance Research Centre'', ''SPbU Computing Centre'', ''Cryogenic Department'', ''Interdisciplinary Resource Centre for Nanotechnology'', ''Centre for X-ray Diffraction Studies'', ''Chemical Analysis and Materials Research Centre'', and ''Centre for Optical and Laser Materials Research'').

FIGURES

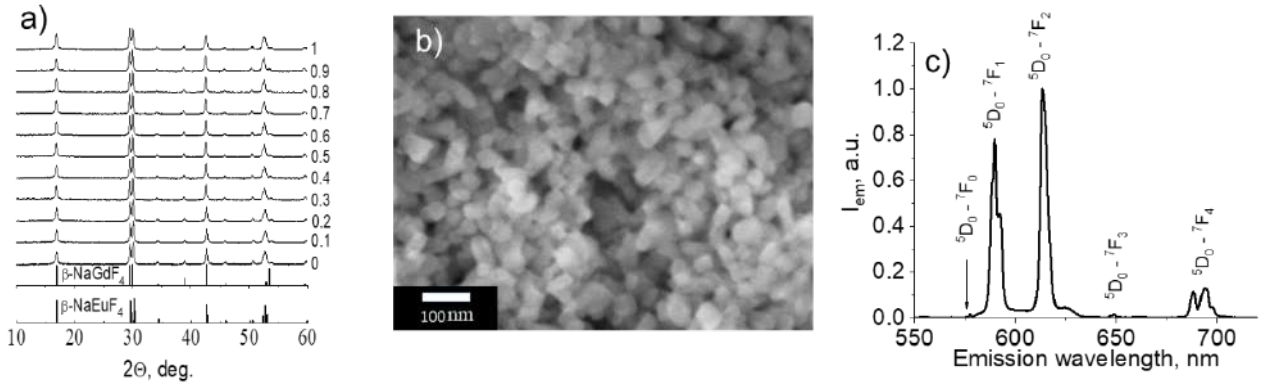

Figure 1. Properties of solid $NaGdF_4$: Eu^{3+} phosphors (a) PXRD patterns (b) SEM image of $NaGd_{0.7}Eu_{0.3}F_4$, (c) emission spectrum of $NaGd_{0.7}Eu_{0.3}F_4$ upon 393-nm excitation

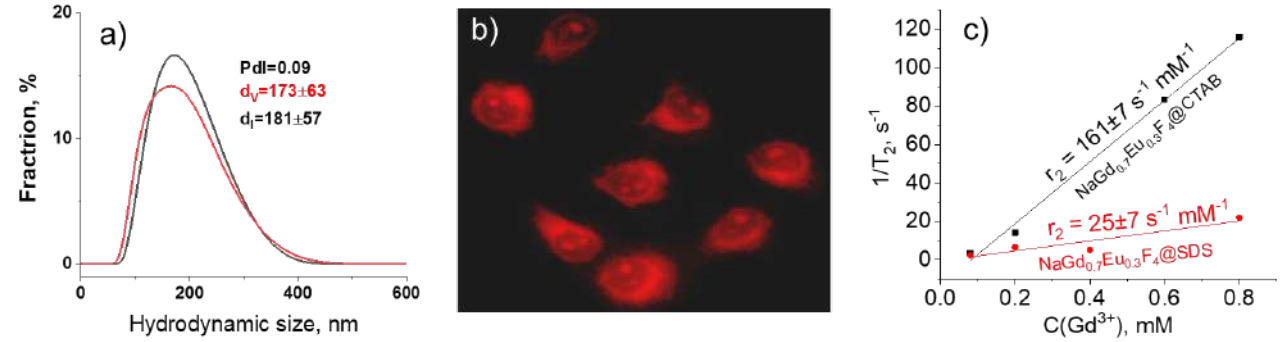

Figure 2. Properties of aqueous solution of surfactant-stabilized $NaGd_{0.7}Eu_{0.3}F_4$ nanoparticles (a) Hydrodynamic size profile and of the CTAB-stabilized $NaGd_{0.7}Eu_{0.3}F_4$ nanoparticles, (b) fluorescence microscopy images M-HeLa cells activated by $NaGd_{0.7}Eu_{0.3}F_4$@CTAB nanoparticles (390 nm excitation, red channel probe, x 400), (c) concentration dependence of $1/T_2$ relaxivity of aqueous solutions of CTAB- and SDS-stabilized $NaGd_{0.7}Eu_{0.3}F_4$ nanoparticles.

Acta Microscopica Vol. 32, Supp. 1, 2023, pp. xx
PROCEEDINGS NSSY 2023- Galapagos 23th-29th April 2023

SYNTHESIS OF SILVER NANOPARTICLES USING EXTRACT OF GERANIUM (PELARGONIUM DOMESTICUM) AND CARRASQUILLA (BERBERIS HALLII), AND ITS USE FOR IMPROVEMENT IN THE GENERATION OF ELECTRICAL ENERGY IN MICROBIAL FUEL CELLS.

Jonathan Escorza (1), Yolanda Angulo (2), Marbel Torres (3)

(1) School of Physical Sciences and Nanotechnology, Yachay Experimental Technology Research University, Urcuquí Ecuador. (2) Center for Nanoscience and Nanotechnology, Universidad de las Fuerzas Armadas ESPE, Sangolquí-Ecuador. (3) Center for Nanoscience and Nanotechnology, Universidad de las Fuerzas Armadas ESPE, Sangolquí-Ecuador
jescorza@yachaytech.edu.ec

In this project, hybrid biological organism was electrically studied using a microbial fuel cell (MFC) prototype of two chambers separated by a salt bridge. The hybrid organism was developed by adhering silver nanoparticles to cyanobacterium Fischerella musicola.

Previous investigations have qualitatively studied the phenolic content in different plants [1], these compounds, also called polyphenols, are substances that contain an aromatic ring with several hydroxyl substituents and due to their polarity they are soluble in water, which gives them different colorations that are altered by their pH[2]. These organic extracts have been used as reducing agents capable of synthesizing precious metal NPs by controlling their size and shape and without having any environmental impact, in what is known as green NP synthesis. The methods by which metallic NPs are manufactured using green sources include phytological (plants and algae), mycological (fungi) and bacteriological synthesis [3].

Previously to the development of the hybrid organism, the growth of the *Fischerella musicola* cyanobacteria was analyzed with different characterization techniques, for this, the photoperiod and gas exchange parameters were controlled, and the temperature and pH of the medium were monitored. Silver nanoparticles (AgNPs) were synthesized by green chemistry using natural extract such as the geranium flower (*Pelargonium domesticum*) and the carrasquilla fruit (*Rhamnus myrtifolius)* to reduce silver nitrate. In the synthesis process, the pH, temperature and time were controlled to obtain nanoparticle sizes of 17.6313 ± 12.6812nm for geranium AgNPs and 24.1294 ± 7.5146nm for carrasquilla ones. These studies showed that, depending on the reducing agent and the synthesis conditions, the shape and size of the nanoparticle differs. Finally, the hybrid organism was developed through the electrostatic adherence of different concentrations of nanoparticles, the AgNPs and the hybrid organisms were characterized by different techniques.

All the studies showed that for a concentration of 2.6mL of AgNPs from Pelargonium domesticum in 20mL of biomass and 40mL of BG11 medium, the best electrical energy generation efficiency was of 0.8043 ± 0.009V and 19.42uA / cm^2, using a two-chamber microbial fuel cell and salt bridge.

REFERENCES

[1] Reyes, N. M. (2018). Análisis de características diferenciales entre antocianinas y betacianinas en extractos de plantas mediante pruebas de color. *Ambiociencias*(16), 38-48.

[2] CreȚU, G., Morlok, G., & Nechifor, G. DEVELOPMENT OF A QUANTITATIVE HIGH PERFORMANCE THIN LAYER CROMATOGRAPHIC METHOD FOR ANALYSIS OF DELPHINIDIN 3-GLUCOSIDE IN BERRY EXTRACTS. Bhattacharya, R., & Mukherjee, P. J. A. d. d. r. (2008). Biological properties of "naked" metal nanoparticles. *60*(11), 1289-1306.

[3] Ramzan, H., & Yousaf, Z. (2018). Chapter 4 - Green fabrication of metallic nanoparticles. In A. M. Grumezescu (Ed.), *Inorganic Frameworks as Smart Nanomedicines* (pp. 137-183): William Andrew Publishing.

FIGURES

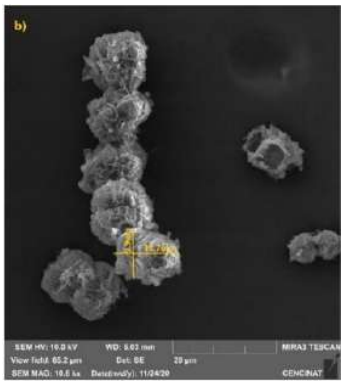

Figure 1. SEM image of Fischerella muscicola

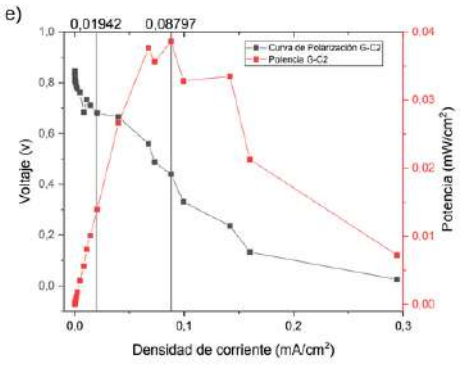

Figure 2. Electrical characterization with MFC of hybrid organisms

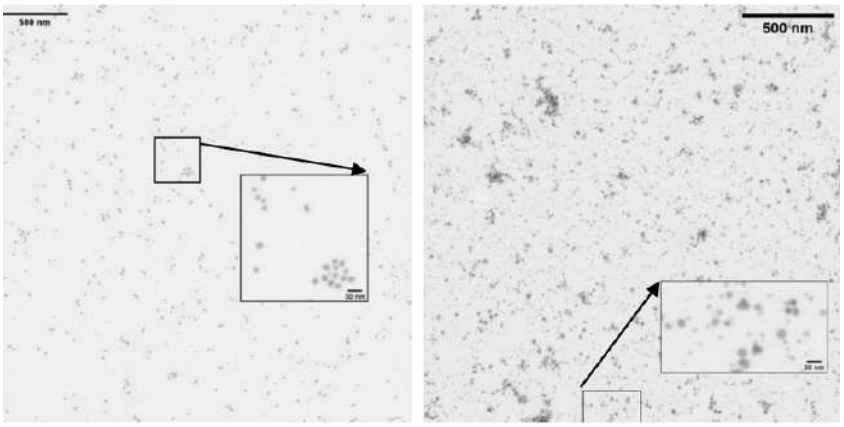

Figure 3. STEM images of AgNPs with Geranium (Right) and Carrasquilla (Left)

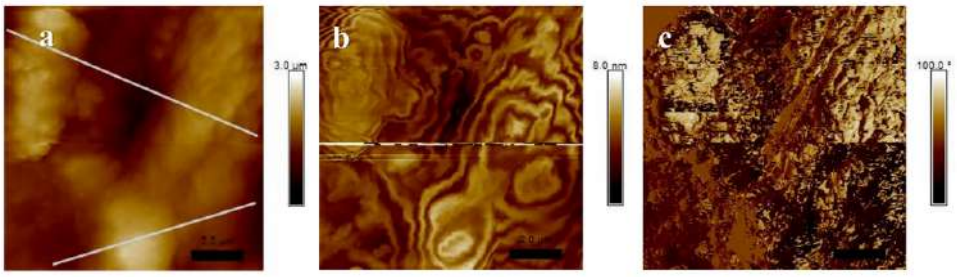

Figure 4. AFM images of electric properties of hybrid organisms

Acta Microscopica Vol. 32, Supp. 1, 2023, pp. xx
PROCEEDINGS NSSY 2023- Galapagos 23th-29th April 2023

DESIGN OF IMPEDANCE COUPLERS FOR GRAPHENE NANOANTENNA IN THE THZ BAND

Manuel Tipán G[a]*, Daniel González T. [b], Johnny Chimborazo [b], Berenice Arguero T[a]* and Germán V.Arévalo [a].

[a] Grupo de Investigación GIETEC, Carrera de Telecomunicaciones, Universidad Politécnica Salesiana, Quito, Ecuador.
[b]School of Physical Sciences and Nanotechnology, Yachay Tech University, Urcuquí, Ecuador.
jchimborazo@yachaytech.edu.ec

The wireless communications of future generations will require nanoantennas capable of working in the band of Terahertz, however, the miniaturization causes difficulties in conductivity, high propagation losses, and degradation in radiation efficiency. In addition, to obtain the maximum power transfer in a nanoscale wireless communication system, impedance couplers are required. Therefore, a graphene-based patch-type nanoantenna was modeled on two dielectric substrates, silicon, and silicon dioxide, in which a BIAS voltage between 0.83 and 29.9 V was applied. For the coupling of the patch with the power port, direct contact methods were used, such as a 50 Ω microstrip line, inserts in the patch, and the quarter-wave transformer.
The best results obtained from the performance comparison were with the quarter wave transformer with a return loss of -33.54 dB, gain 5.6 dBi, directivity 6.05 dBi, VSWR of 1.15, a bandwidth of 350 GHz, efficiency of 92%, HPBW 99.2°, F/B 12.8 dB for a resonance frequency of 2.6 THz and in the case of 4.2 THz a return loss of -35.24 dB, gain 4.9 dBi, directivity 5.6 dBi, VSWR of 1.13, bandwidth 187 GHz with 90% efficiency, HPBW 106.5°, F/B 12.2 dB. So, the quarter wave transformer is optimal for matching impedances, achieving low propagation losses, and complying with the optimal operating parameters.

REFERENCES

1 J. N. George, M. G. Madhan, Physica E: Low-dimensional Systems and Nanostructures, vol. 94, pp. 126–131, 2017.

2 J. M. Shalini, M. G. Madhan, Optik (Stuttg), vol. 194, p. 163050, 2019.

3 I. Llatser, C. Kremers, A. Aparicio, J. M. Jornet, E. Alarcón, D. N. Chigrin, *Photonics and Nanostructures - Fundamentals and Applications*, vol. 10, no. 4, pp. 353–358, 2012.

4 S. Abadal, S. E. Hosseininejad, A. Aparicio, E. Alarcon, *2017 40th International Conference on Telecommunications and Signal Processing (TSP)*, Jul. 2017, pp. 817–820.

FIGURES

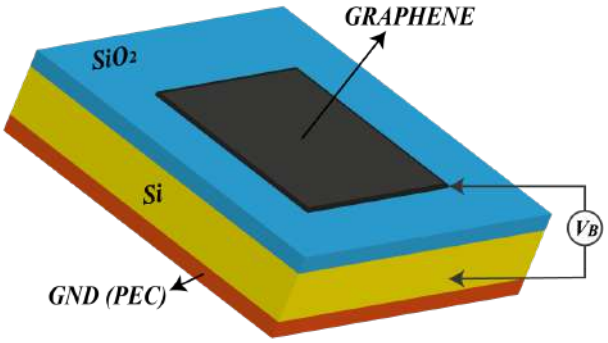

Figure 1. Nanoantenna Components

Table 1: Characteristics of the dielectrics and ground plane of the nanoantenna.

Parameter	Substrate 1	Substrate 2	GND
Material	Silicon	SiO_2	
Er	11,9	4	
Loss Tan∂	0,009	0,005	PEC
Thickness	1.5/1.57 [um]	0.025 [um]	

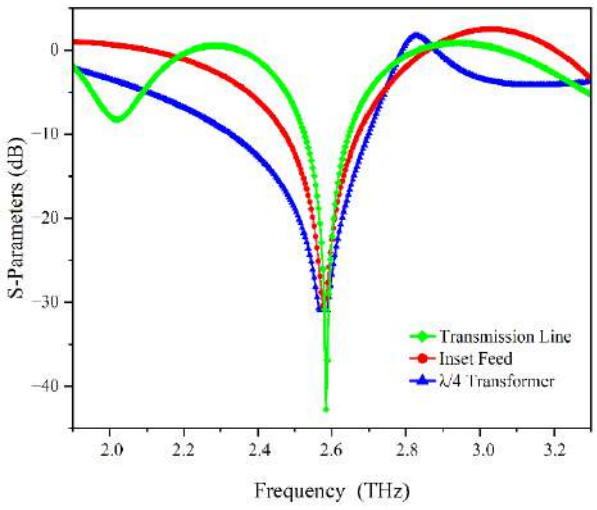

Figure 2. S-Parameters at 2.6 THz.

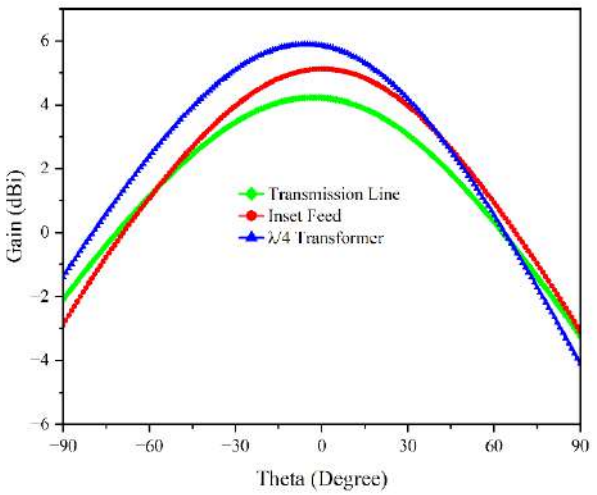

Figure 3. Gain at 2.6 THz.

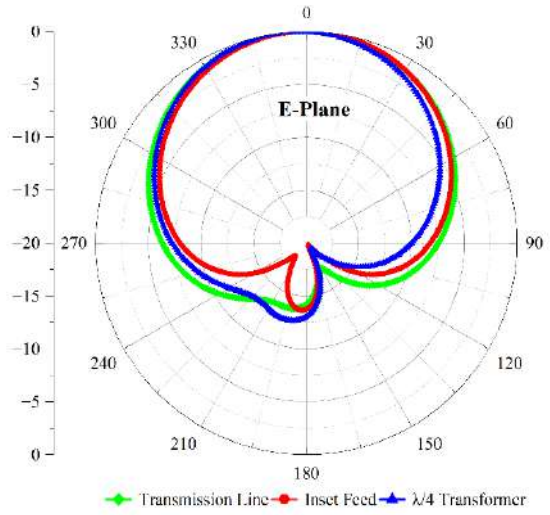

Figure. 4. Radiation pattern at a frequency of 2.6 THz.

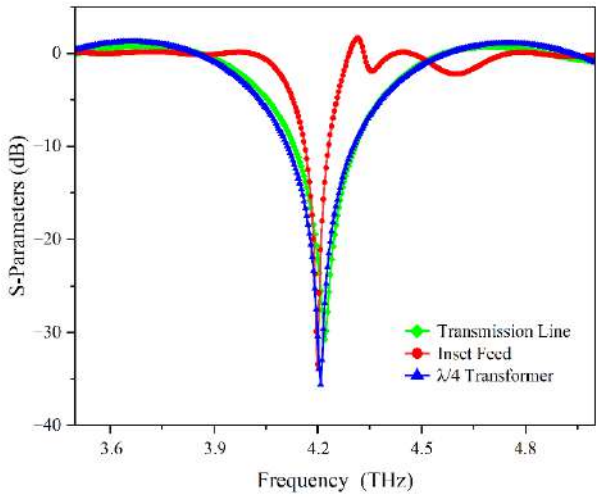

Fig. 5. S-Parameters at 4.2 THz.

TUESDAY

Molecular Modelling of Nanostructures

Acta Microscopica Vol. 32, Supp. 1, 2023, pp. xx
PROCEEDINGS NSSY 2023- Galapagos 23th-29th April 2023

SCANNING THE ELECTROMAGNETIC EIGEN-MODES IN LAYERED VAN DER WAALS HETEROSTRUCTURES

Vito Despoja(1,2) and Neven Golenić(3,4)

(1)Institute of Physics, Bijenička 46, 10000 Zagreb, Croatia
(2) Donostia International Physics Center (DIPC), P. Manuel de Lardizabal, 4, 20018 San Sebastián, Spain
(3)Department of Physics, Faculty of Science, University of Zagreb, Bijenička 32, 10000Zagreb, Croatia
(4)Scuola Internazionale Superiore di Studi Avanzati (SISSA), Via Bonomea 265, 34136 Trieste, Italy
vito@phy.hr

Recently, the electromagnetic modes in atomically thin van der Waals (vdW) layered heterostructures have shown great potential for their practical applications in plasmonics, photonics and optoelectronics. For example, by vertical stacking of various transition metal dichalcogenides (TMDs), hexagonal boron nitride (hBN) and graphene (Gr) the heterostructure of varous optical properties can be achieved which can act as a photo-sensor, photovoltaic or photo-emitter [1,2,3]. Here we present the results of our recently proposed theoretical approach [4], which is applied to study the electromagnetic eigen-modes in layered conducting and semiconducting van der Waals (vdW) heterostructures. Obtained results for diverse and tunable *Dirac plasmon - polaritons* ((DPP) in Gr/hBN and Gr/$FeCl_3$ multilayers will be presented and compared with recent Scanning Near-Field Microscopy (SNOM) measurements. The occurrence of exotic, transversal polarisation mode (called *trapped photon*) in semiconducting vdW heterostructures will be demonstrated [5,6]. The *trapped photon* (T-ph), built from inter-band electron-hole excitations (not necessarily from excitons) and the transversal photons, is the transversal counterpart to DPP in conductive 2D materials, built from intra-band electron-hole excitations and the longitudinal photons. **Figures 1(a-d)** show the results for T-ph normalised oscillatory strengths f_x/N in WS_2/hBN multilayers and compare with normalised oscillatory strengths $f_{x,y}/N$ of T-ph and DPP in Gr/hBN multilayers. We obtained that T-ph in WS_2/hBN bilayer (N=2) is 29 times stronger then T-ph and even 7 times stronger than DPP in heavily doped ($n=10^{14}cm^{-2}$) Gr/hBN bilayer **Fig.1(c)**. We present the results for T-ph intensity in WS_2/hBN multilayers, in (**Q**,ω) and spatial **ρ**=(x,y) space simulating the SNOM measurements. **Figures 1 (e)** and **(f)** show the SNOM simulations of T-ph and DPP in WS_2/hBN and in doped Gr/hBN trilayers, respectively.

REFERENCES

[1] F. Bonaccorso, Z. Sun, T. Hasan and A. C. Ferrari, Nature Photon 4, 611 (2010)
[2] L. Britnell, et al, Science 340, 1311 (2013)
[3] J. Wang, X. Mu, M. Sun b, T. Mu, Applied Materials Today 16, 1-20 (2019)
[4] D. Novko, K. Lyon, D. J. Mowbray, and V. Despoja, Phys. Rev. B 104, 115421 (2021)
[5] S. A. Mikhailov and K. Ziegler Phys. Rev. Lett. 99, 016803 (2007)
[6] V. Despoja and L. Marušić, Int. J. Mol. Sci. 23, 6943 (2022)

ACKNOWLEDGMENTS

The authors acknowledge financial support from Croatian Science Foundation (Grant no. IP-2020-02-5556) as well as from European Regional Development Fund for the "QuantiXLie Centre of Excellence" (Grant KK.01.1.1.01.0004).

FIGURES

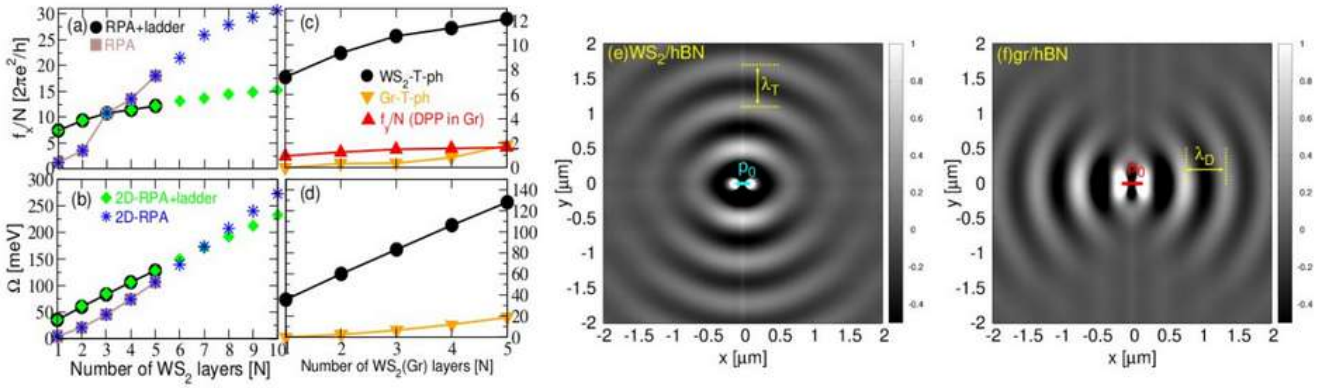

Fig.1 (a) The T-ph normalised oscillatory strength f_x/N and (b) bending Ω as a function of the number of WS_2 single-layers (N) in WS_2/hBN heterostructure obtained using (●) RPA+ladder, (■) RPA, (◆) 2D-RPA+ladder and (★) 2D-RPA models. (c) The T-ph oscillatory strength f_x/N in (●) WS_2/hBN, in (▼) Gr/hBN and (▲) DPP oscillatory strength f_y/N in Gr/hBN multilayers. (d) The T-ph bending Ω in (●) WS_2/hBN and in (▼) Gr/hBN multilayers. (e) The induced current $j^{ind}_x(\boldsymbol{\rho})$ in WS_2/hBN and in (f) graphene/hBN trilayers driven by point dipole $\mathbf{p}$=(1,0) ocillating at frequencies ω_T=1.957eV and ω_D=0.29eV, respectively. The graphene electron doping is $n=10^{14}cm^{-2}$ per Gr layer corresponding the Fermi level shift of E_F=1eV.

Acta Microscopica Vol. 32, Supp. 1, 2023, pp. xx
PROCEEDINGS NSSY 2023- Galapagos 23th-29th April 2023

SAFE AND SUSTAINABILITY-BY-DESIGN: CHALLENGES AND ADVANCED IN COMPUTATIONAL DESIGN OF ADVANCED MATERIALS

Alicja Mikolajczyk (1, 2)

(1) [a] Laboratory of Environmental Chemoinformatics, Faculty of Chemistry, University of Gdansk, Wita Stwosza 63, 80-308 Gdańsk, Poland, (2) QSAR Lab Sp. Z o. o., Trzy Lipy 3, 80-172, Poland
fourth author. Times New Roman 10 pt, centered. All Affiliations must include Department/Institution, City and Country.
alicja.mikolajczyk@ug.edu.pl

Engineered nanomaterials (ENMs) enable new and enhanced products and devices in which matter can be controlled at a near-atomic scale (in the range of 1 to 100 nm). However, the unique nanoscale properties that make ENMs attractive may result in as yet poorly known risks to human health and the environment. Thus, new ENMs should be designed in line with the idea of safe-and-sustainable-by-design (SSbD). The biological activity of ENMs is closely related to their physicochemical characteristics, changes in these characteristics may therefore cause changes in the ENMs activity. In this sense, a set of physicochemical characteristics (for example, chemical composition, crystal structure, size, shape, surface structure) creates a unique 'representation' of a given ENM. The usability of these characteristics or nanomaterial descriptors (nanodescriptors) in nanoinformatics methods such as quantitative structure–activity/property relationship (QSAR/QSPR) models, provides exciting opportunities to optimize ENMs at the design stage by improving their functionality and minimizing unforeseen health/environmental hazards. A computational screening of possible versions of novel ENMs would return optimal nanostructures and manage ('design out') hazardous features at the earliest possible manufacturing step. Safe adoption of ENMs on a vast scale will depend on the successful integration of the entire bulk of nanodescriptors extracted experimentally with data from theoretical and computational models. This Review discusses directions for developing appropriate nanomaterial representations and related nanodescriptors to enhance the reliability of computational modelling utilized in designing safer and more sustainable ENMs.

REFERENCES

[1] Wyrzykowska E., Mikolajczyk A., et al. *Nature Nanotechnology*, **17**, pages924–932 (2022)

ACKNOWLEDGMENTS

This work has received funding from the European Union's Horizon 2020 research and innovation program under grant agreement No 814426 (NanoInformaTIX project), No 953152 (DIAGONAL project) and No 101058784 (NOVUEAU project).

Acta Microscopica Vol. 32, Supp. 1, 2023, pp. xx
PROCEEDINGS NSSY 2023- Galapagos 23th-29th April 2023

PHOTOINDUCED QUANTUM TRANSPORT

Duncan J. Mowbray (1), Jeyson P. Alomoto-Catota (1), Daniel E. Gonzalez Tamayo (1), Vito Despoja (2)

(1) School of Physical Sciences and Nanotechnology, Yachay Tech University, Urcuqui 100119, Ecuador. (2) Institute of Physics, 10000 Zagreb, Croatia.
duncan.mowbray@gmail.com

A commonly used metric for rating solar cells is their external quantum efficiency (EQE), which is the fraction of incident photons of a particular energy that generate charge carriers. Although this ignores both the power produced by those charge carriers and the availability of photons of that energy in the solar spectrum, it provides a balanced, simple, and general method for comparing photovoltaic materials on a common footing. For this reason, efficient ab initio methods that can semi-quantitatively describe a material's EQE are needed. To do so, the material's optical absorption, charge carrier generation, and the resulting charge transport at a quantum level are needed to describe the EQE of a photovoltaic device. Here, we extend the non-equilibrium Green's function formalism to describe the entire photoinduced quantum transport process within a device, as depicted schematically in Figure 1. This method provides an efficient means for estimating the EQE of photovoltaic devices, allowing their design in silico.

FIGURES

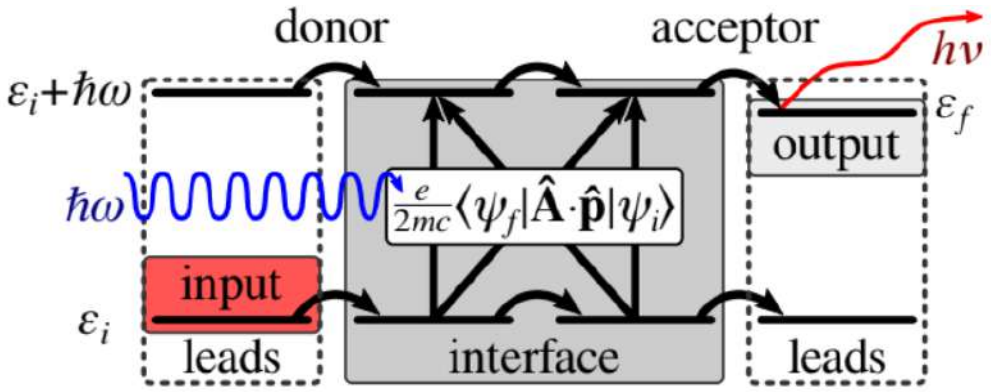

Figure 1. Schematic of an excitation process across a donor–acceptor interface from an occupied initial state in the input lead to an unoccupied intermediate state via the interaction between an external electromagnetic field with vector potential Â and momenta p and via coupling to a phonon mode to an unoccupied final state in the output lead.

Acta Microscopica Vol. 32, Supp. 1, 2023, pp. xx
PROCEEDINGS NSSY 2023- Galapagos 23th-29th April 2023

ELECTRONIC AND SPIN TRANSPORT IN MOLECULAR JUNCTIONS

Carlos Sabater

Departamento de Física Aplicada and Instituto Universitario de Materiales de Alicante (IUMA), Universidad de Alicante,Campus de San Vicente del Raspeig, E-03690 Alicante, Spain.
carlos.sabater@ua.es

Atomic or molecular contacts have always been an excellent testing bench for the study of electronic and spin transport. Additionally, when the contact is formed by a single atom or molecule, it becomes more interesting since we can obtain mechanical, electrical, and magnetic properties for this unique element. The electronic transport approach is usually studied through Break-Junctions (BJ) experiments, with the most common techniques being Scanning Tunneling Microscopes (STM-BJ) and Mechanically Controllable Break Junctions. On the other side, it is common in theoretical studies to use molecular dynamics (MD) simulations to obtain the trajectories of all atoms or molecules when emulating an experiment, or ab initio calculations based on Density Functional Theory (DFT) when calculating electronic transport.
Our research focuses on studying quantum transport in atomic and molecular conductors. We employ a variety of techniques to investigate this phenomenon, including STM-BJ and MCBJ experiments, MD simulations, and electronic transport calculations based on DFT. Depending on the requirements of each experiment, we can perform measurements at either cryogenic or room temperature conditions. Recently, we have incorporated spin-lattice simulations [1] into our MD models, and our DFT calculations count with the implantation of the spin-orbit coupling effect [2].
Here we present our experimental and theoretical results on electronic and spin transport in atomic contacts.
Thanks to our theoretical-experimental findings in bilayers of bismuth (111), we detected the Quantum Spin Hall insulator behavior at room conditions [3]. Furthermore, our experimental and theoretical results on nickel nanocontacts explain how the electronic transport is affected by the presence of magnetic domains [1].
Regarding molecular electronics-spintronics, we have two important messages to share. First and foremost, our theoretical-experimental results show that organic solvents play a role in molecular electronics. Our findings demonstrate that some solvents never fully evaporate, and their electronic transport must be considered [4,5]. Secondly, we present our experimental and theoretical results in molecular electronic-spintronics based on the Chiral Induced Spin-Selectivity (CISS) effect. Our results on dithiahelicene molecules (see figure 1) demonstrate an interesting behavior in electronic transport experiments [6,7]. We also have used DFT to calculate electronic and spin transport for the previously mentioned molecules, and our theoretical results lead to new questions and insights on the CISS effect. Moreover, our computational results have revealed that non-magnetic metallic nanocontacts can exhibit spin polarization when a rotation is introduced in the electrodes (see figure 2), in other words, the CISS effect can be produced without chiral molecules and can be explained by a matter of symmetry [2].
In summary, based on our findings, we present here an improvement in the understanding of electronic and spin transport in single atomic and molecular junctions.

REFERENCES

[1] Dednam W. et al. Phys. Rev. B. (2020) (102) (245415).
[2] Dednam W. et al. ArXiv.(2022) (arXiv:2211.04830v2).
[3] Sabater C. et al Phys. Rev. Lett. (2013) (110) (176802).
[4] de Ara T. et al. Mat. Chem. Phy. (2022) (291) (126645).
[5] Martinez-Garcia A. et al. ArXiv. (2023) (arXiv:2302.08389v1).
[6] Baciu B. et al. Nanoscale Adv. (2020) (2) (1921).
[7] Baciu B. et al. J. Mater. Chem. C. (2022) (10) (14306).

ACKNOWLEDGMENTS

This work was supported by the Generalitat Valenciana through CIDEXG/2022/45, CIGRIS/2021/159, CDEIGENT/2018/028, and PROMETEO/2021/017.

FIGURES

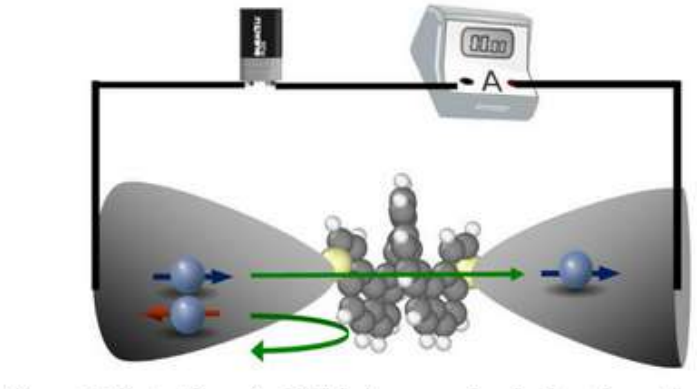

Figure 1. Illustration of a dithiahelicene molecular junction acting as a spin filter.

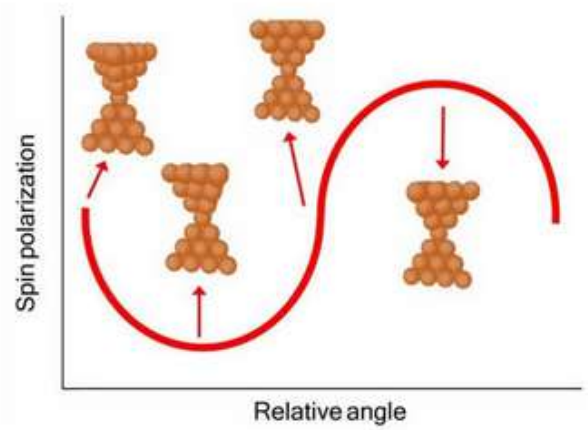

Figure 2. Illustration of spin polarization varies the relative angle between electrodes in atomic-sized contact.

Acta Microscopica Vol. 32, Supp. 1, 2023, pp. xx
PROCEEDINGS NSSY 2023- Galapagos 23th-29th April 2023

CVD GROWTH AND GAS SENSING PROPERTIES OF METAL OXIDE AND TRANSITION METAL DICHALCOGENIDE MATERIALS

Fatima Ezahra Annanouch (1) Èric Navarrete Gatell (1), Carla Bittencourt (2) and Eduard Llobet (1)

(1) Universitat Rovira i Virgili, Electronic Engineering, Avda. Països Catalans, 26, 43007 Tarragona, Catalonia, Spain.
(2) Plasma-Surface Interaction Chemistry, Chemistry Department, University of Mons, Mons, Belgium.
eduard.llobet@urv.cat

Year by year, gas sensors have known tremendous developments in terms of sensing materials, size, power consumption and fabrication costs. They are becoming indispensable items in the monitoring of indoor and outdoor toxic gasses, and thus play an increasing role in environmental monitoring, air quality control or in safety and security applications. Exposure to high concentrations of toxic gasses is a serious health threat [1]. Hence, developing a new generation of gas sensors that can monitor such pollutant gasses in real time and can detect concentrations from as low as a few parts per billion to several hundred parts per million in the air is of a strong industry demand. In this context, chemiresistive sensors based on nanostructured metal oxide semiconductors, such as WO3, ZnO, SnO2 and In2O3, only to cite a few have been extensively used for detecting pollutant gasses, owing to their advantages of sensitivity, low cost, simple fabrication process and reliability. They were launched as building block materials for gas sensors, owing to their high surface-to-volume ratio, low number of defects, electron confinement effect, etc. In the first part of my lecture, I will describe how pristine and metal nanoparticle loaded metal oxide nanowires (see Figure 1, top row) can be grown via the aerosol-assisted chemical vapor deposition and I will discuss their gas sensing properties and will also introduce their gas sensing mechanisms [2,3]. Lack of selectivity and humidity cross-sensitivity remain the major drawbacks to overcome in metal oxides. Additionally, these nanomaterials are normally operated at 100–400 °C, leading to high power consumption and reduced sensor stability and lifetime, owing to thermally induced changes in morphology and poisoning effects.
These drawbacks are limiting the adoption of metal oxide nanomaterial chemiresistors in the wider real-time applications. In a quest for overcoming such drawbacks, researchers have recently drawn towards atomically layered two- dimensional (2D) transition metal dichalcogenide (TMDs) nanomaterials. TMDs possess unique properties such as semiconducting properties, direct band gap, high specific surface areas due to their sheet-like structures with large basal planes and highly-reactive edges. TMDs consist of a metal atomic layer (such as Mo, W, Hf, Ti, Zr, V, Nb, Ta, Re, etc) collocated between two chalcogen atomic layers (S, Se or Te) and then, these 2D trilayers may appear stacked in multilayer structures due to van der Waals interactions. In the second part of my lecture I will report the bottom-up synthesis of pure and metal oxide loaded transition metal di-chalcogenides (TMDs) such as WS2, WSe2, MoS2 employing different chemical vapor deposition (CVD) methods. These materials comprise ultra-thin films and 3D assemblies of vertically-aligned TMD (see Figure 1, bottom row) nano-flakes and nano-triangles (pristine or loaded with metal/ metal oxide nanoparticles). These materials are grown directly onto application substrates with interdigitated electrodes for achieving chemo-resistive devices [4-6]. The morphological, structural and chemical characteristics will be discussed by using FESEM, TEM, EDX and XPS analysis. Full gas sensing studies towards toxic gases and vapors such as nitrogen dioxide, hydrogen sulfide and ammonia will be shown and discussed as well. These will comprise sensitivity, selectivity, limits of detection, moisture cross-sensitivity effects and long term stability. The effects of the operating temperature on sensitivity and baseline recovery will be addressed. Finally, gas sensing mechanisms will be presented and discussed in detail.

REFERENCES

[1] Occupational Safety and Health Administration, Permissible Exposure Limits – Annotated Tables https://www.osha.gov/annotated-pels/table-z-1 (accessed Nov 10, 2022).
[2] Annanouch, F.E. et al. ACS Appl. Mater. Interfaces 2016, 8 (16).
[3] Annanouch, F.E. et al. ACS Appl. Mater. Interfaces 2015, 7 (12).
[4] Alagh, A. et al. Sensors Actuators B: Chem. 2021, 326, 128813.

[5] Annanouch, F.E. et al. J. Mat, Chem C. J. Mater. Chem. C, 2022,10, 11027-11039.
[6] Alagh, A. et al. ACS Appl. Mater. Interfaces. 2022, 14, 49, 54946–54960.

ACKNOWLEDGMENTS

Funded in part by the Marie Skłodowska-Curie Actions (MSCA) Research and Innovation Staff Exchange (RISE)H2020-MSCA-RISE- 2018- 823895 'SENSOFT', by MICINN and FEDER grant no. RTI2018-101580-I00 and AGAUR grant no.2017 SGR 418. C.B. is Senior Research Associate of the national funds for Scientific Research (FRS-FNRS, Belgium). E.L. is supported by the Catalan Institute for advanced studies (ICREA) via the 2018 Edition of the ICREA Academia Award.

FIGURES

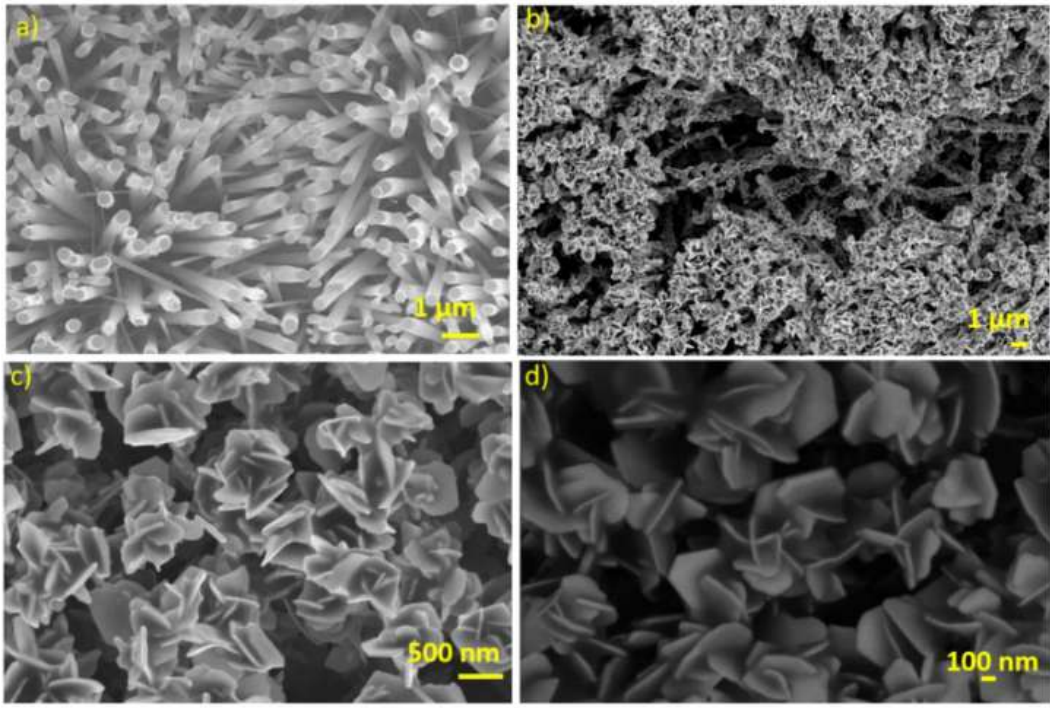

Figure 1. SEM and FESEM images depicting the growth of vertically aligned (a) WO3 nanowires (b) WSe2 nanoplatelets (c) (d) WSe2 nanoflowers. Reproduced from [6]. American Chemical Society.

WEDNESDAY

2D Nanomaterials and Heterostructures

Acta Microscopica Vol. 32, Supp. 1, 2023, pp. xx
PROCEEDINGS NSSY 2023- Galapagos 23th-29th April 2023

WHY FILLED SINGLE-WALLED CARBON NANOTUBES

Paola Ayala (1)

(1) University of Vienna, Faculty of Physics, A1090 Vienna, Austria
paola.ayala@univie.ac.at

The advances on the science and application of carbon nanotubes within the last three decades have brought to reality the production of materials approaching the theoretical predictions. In particular, the outstanding electronic and optical properties of pristine single-walled carbon nanotubes can be clearly unraveled with more than one spectroscopy technique. However, seeking paths to gain control and modify the material´s properties implies understanding interactions of the SWCNTs with other structures or molecules. This is why unraveling the properties of hybrids of SWCNTs, where they encapsulate other structures, still embraces significant challenges. The physical properties of these materials are strongly related to their morphology and diameter. For instance, their photoluminescence (PL) can be modified by molecules or nanostructures inside the tube´s hollow core. This has been observed for bundles or relatively large- diameter tubes. However, small diameter tubes can form novel hybrids confining linear carbon chains or some types of nanoribbons that offer extremely attractive properties. In this presentation, I will show how our efforts towards identifying the charge transfer from encapsulated nanostructures to SWCNT hosts on hybrids confining linear carbon chains and given chirality nanoribbons. We will discuss the extraction of SWCNT-carbon chain-hybrids protected inside their double-walled counterparts, and on how a diameter-dependent enhancement of the PL can be induced by energy transfer. Also, graphene nanoribbons with a defined chirality will be in the focus of this presentation showing how to discern specific Raman active modes independently from non-encapsulated fragments of ribbon-like molecules.

REFERENCES

[1] Milotti V. et al. *Small Methods*, (2022) (6) (2000110).
[2] Rohringer, P. et al *Adv. Funct. Mater*. (2016) (26) (4874).
[3] Denvier van der Gon D. et al. *Manuscript in preparation* (2023)

ACKNOWLEDGMENTS

P. Ayala acknowledges the fruitful collaboration on the presented topics with Thomas Pichler (University of Vienna-Austria), Kazuhiro Yanagi (Tokyo Metropolitan University-Japan), Lei Shi (Sun Yat-sen University-China), Valeria Milotti (ELETTRA-Italy), Manuel Melle Franco and Jorge Laranjeira (University of Aveiro-Portugal). Also the work of the PhD Students of the Tailored Hybrid Structures Group C. Berkmann, D. Denvier van der Gon, J. Benalcázar is kindly acknowledged.

Acta Microscopica Vol. 32, Supp. 1, 2023, pp. xx
PROCEEDINGS NSSY 2023- Galapagos 23th-29th April 2023

MOLECULARLY DESIGNED 2D MATERIAL ARCHITECTURES: A ROUT TOWARSD APPLICATIONS

Mildred Quintana[1,2]

Facultad de Ciencias[1] and Centro de Investigación en Ciencias de la Salud y Biomedicina (CICSaB)[2],
Universidad Autónoma de San Luis Potosí.
mildred.quintana@uaslp.mx

2D materials namely graphene, MoS_2, WS_2, borophene, black phosphorus, hexagonal boron nitride, etc, are exciting materials with a huge potential for the development of new advanced technologies. The unique combination of properties, such as high specific surface area, chemical stability, mechanical strength, flexibility, high electrical and thermal conductivity, and tunable band gap, make them ideal components for the development of several applications including intelligent coatings, conductive inks, reinforced composites, biomedical devices, smart membranes, and environmentally friendly materials. However, for applicability, several problems arise, including scalability, dispersibility and stability. Authors have proposed chemical functionalization as a feasible solution to render 2D materials dispersible in many solvents and readily for its integration in different matrices. Furthermore, by performing chemical reactions, it is possible to exactly tune the interfacial properties to increase compatibility and integration into functional composites. In this presentation, I will describe our recent efforts on the chemical functionalization of 2D materials towards applications.

FIGURES

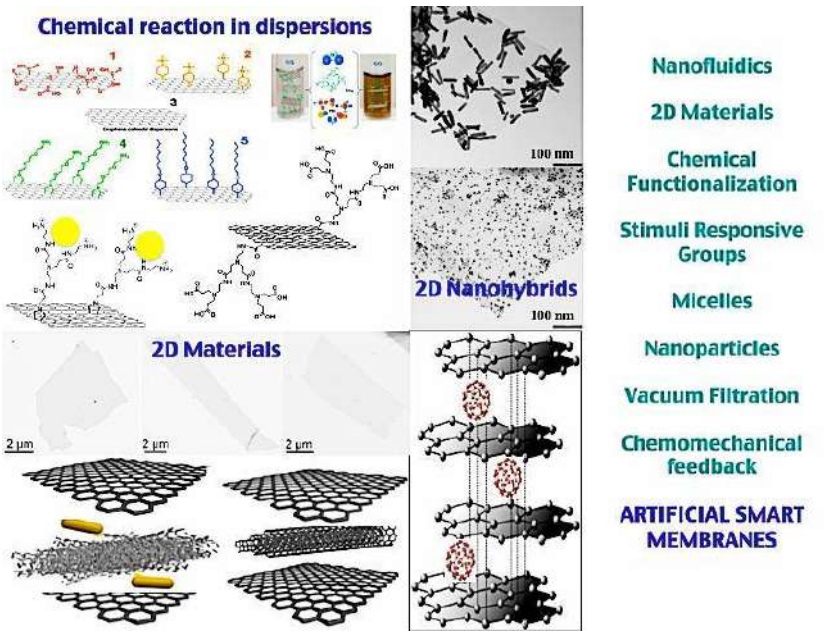

Figure 1. Schematic representation of the chemical functionalization of 2D materials.

Acta Microscopica Vol. 32, Supp. 1, 2023, pp. xx
PROCEEDINGS NSSY 2023- Galapagos 23th-29th April 2023

2D NANOELECTRODES FOR SINGLE MOLECULE JUNCTIONS

Hillary Rodríguez (1), Selena Barragán (1), Yessenia Falconí (1), Pedro Ortiz (1), Henrry M. Osorio C. (1)
(1) Electronic and magnetic materials group (GI-MEM), Departamento de Física, Escuela Politécnica Nacional. Av. Ladrón de Guevara, E11-253, 170525 Quito, Ecuador.
henrry.osorio@epn.edu.ec

Molecular electronics, in which organic, inorganic or organometallic molecules are connected between two (or three) electrodes to create a nascent electronic device has potential to serve a role in the development of a new technology that could overcome the difficulties now being encountered during top-down scaling of conventional silicon technology. The development and evolution of several experimental techniques, such as scanning tunneling and atomic force microscopies, have enabled us to evaluate the electrical properties across metal-molecule-metal junctions. Together with these techniques, metallic electrodes, especially gold, have been extensively used to address key interrogations related to understanding charge transport mechanisms across the junctions or to propose novel structures to construct molecular diodes or, even better, molecular transistors. However, there are potential drawbacks of using metallic electrodes for the assembly of these junctions, such as: non-compatibility with complementary metal-oxide-semiconductor (CMOS) technologies, surface mobility and high price. Over the last years, the use of non-metallic electrodes has attracted growing attention due to avoiding the use of rare, expensive and potentially toxic materials. Thus, graphene,[1] molybdenum disulfide (MoS2) [2] or gallium arsenide (GaAs) [3] nanoelectrodes have been successfully used to obtain molecular junctions with inherent properties, such us, low attenuation factors, photocurrent or current rectification. Nevertheless, these contacts need expensive methods for deposition or to provide optimal electrical contact. In this talk, I will describe our efforts to construct and characterize molecular junctions based on 2D non-metallic electrodes in a simple way using scanning probe microscopy. Thus, electrical properties of graphene-molecule-gold and MoS2-molecule-gold junctions will be examined. In the first case, multilayer graphene nanosheets were obtained using electrochemical exfoliation of graphite. Subsequently, spray-coated graphene electrodes were constructed from graphene nanosheets. In the second case, multilayer MoS2 nanosheets were obtained using liquid-phase exfoliation of MoS2 powder and after deposited using a drop-casting method to construct a semiconducting electrode. Atomic force microscopy (AFM) was used to evaluate the morphology of the deposited electrodes and scanning tunneling microscopy (STM)-based I(s) method was performed to construct and evaluate the conductance of graphene-molecule-gold and MoS2-molecule-gold junctions. In both cases, the single molecule I-V curve of 4,4'-biphenyldithiol was obtained. A symmetrical I-V curve was obtained for the graphene-molecule-gold junction (Figure 1a), proving that, despite the inherent asymmetry of the molecular junction, no rectification effect was detected. On the other hand, MoS2- molecule-gold junction exhibited an asymmetrical I-V curve (Figure 1b). This indicates the establishment of current rectification, which is related to the asymmetry created with the use of different electrodes to form the junction. In summary, this study paves the way for the use of nanoelectrodes based on 2D-materials to construct single molecule junctions and evaluate charge transport at the molecular level. Importantly, with the use of MoS2 semiconducting nanoelectrodes current rectification is promoted at the molecular level.

REFERENCES

[1] Zhao, S., et al. Nano Research (2021) (1).
[2] Eo, J. S., et al. Advanced Science (2021) (8) (2101390).
[3] Vezzoli, A., et al. Nano Letters (2017) (17) (1109).

ACKNOWLEDGMENTS

Authors are grateful for financial assistance from Escuela Politécnica Nacional in the framework of project PIGR-19-04. In addition, authors thank CEDIA for founding I+D+i-XVII- 2023-48.

Acta Microscopica Vol. 32, Supp. 1, 2023, pp. xx
PROCEEDINGS NSSY 2023- Galapagos 23th-29th April 2023

FIGURES

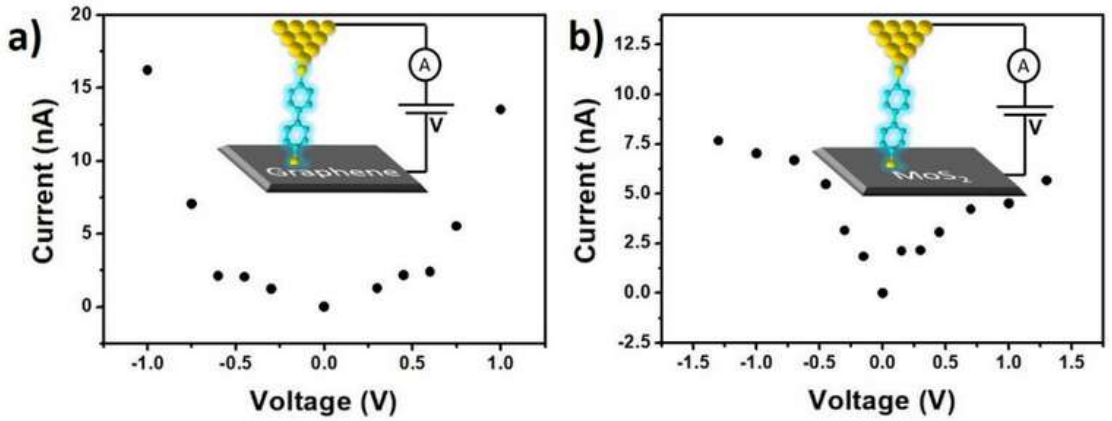

Figure 1. Single molecule I-V curves of 4,4'-biphenyldithiol contacted between two electrodes. a) Graphene-molecule-gold junction and b) MoS2-molecule-gold junction.

Acta Microscopica Vol. 32, Supp. 1, 2023, pp. xx
PROCEEDINGS NSSY 2023- Galapagos 23th-29th April 2023

RAMAN SPECTROSCOPY: INNOVATIVE SAMPLE SCANNING METHODS, ARTIFICIAL INTELLIGENCE CHEMOMETRICS, IMAGE MICROGEOPROCESSING AND COLOCALIZED MEASUREMENTS WITH SCANNING ELECTRON MICROSCOPY AND X-RAY MICROFLUORESCENCE.

Igor Carvalho (1), Filipe Cabral (1)
(1) Horiba Scientific Brazil, Jundiai – São Paulo, Brazil.
igor.carvalho@horiba.com

This presentation will focus on Raman and NanoRaman applied to the most diverse branches of knowledge. In this presentation you will learn the basic principles of Raman spectroscopy applied to Raman imaging. Applications and instrumentation will be the main topics for a wide range of materials characterization, including polymers, ceramics, biomaterials, life sciences and two-dimensional (2D) materials. Raman and Nanoraman microscopy is one of the only techniques capable of providing non-destructive, accurate analysis combined with high resolution images. Raman spectroscopy provides valuable information about the studied sample, such as chemical and structural composition. Based on the light-matter interaction, we obtain relevant information, such as: particle distribution, homogeneity, grain size, phase changes and several other characteristics of the sample through the chemical evaluation of the material. We will also discuss the combination of laser-excited photoluminescence imaging and Raman scattering of two-dimensional (2D) crystals to reveal the solid-state structure. The development of instrumentation makes possible the hyphenation of Raman with other techniques, such as Photoluminescence and AFM, being able to reach resolutions on a nanometric scale. The technique can be applied in several areas of knowledge, such as pharmaceuticals, photovoltaics, graphene, cells, nanoparticles, microplastics, among others.

Acta Microscopica Vol. 32, Supp. 1, 2023, pp. xx
PROCEEDINGS NSSY 2023- Galapagos 23th-29th April 2023

DESIGN OF A MULTIFUNCTIONAL NANOSTRUCTURED SYSTEM WITH POTENTIAL APPLICATIONS IN BREAST AND CERVICAL CANCER TREATMENT

Verónica Quilumba-Dutan (1)*, Clara Carreón-Álvarez (2), Sergio Hidalgo-Figueroa (3), Rubén López-Revilla (4), Eugenia Valsami-Jones (5), Swaroop Chakraborty (6), José Luis Rodríguez-López (7)

(1), (7) Advanced Materials Department,
Instituto Potosino de Investigación Científica y Tecnológica, San Luis Potosí, México.
(2) Departamento de Ciencias Naturales y Exactas
Centro Universitario de los Valles, Universidad de Guadalajara, Jalisco, Ameca, México.
(3), (4) Molecular Biology Department, Instituto Potosino de Investigación Científica y Tecnológica, San Luis Potosí, México. (5), (6) School of Geography, Earth, and Environmental Sciences
University of Birmingham, Birmingham, United Kingdom
veronica.quilumba@ipicyt.edu.mx

In 2020, 19.3 million new diagnosed cases of cancer and 10 million cancer deaths were estimated worldwide. Moreover, an estimated 28.4 million new cancer cases are projected to occur in 2040. Particularly, breast and cervical cancers are the most diagnosed cancers and the major cause of cancer deaths in women.[1] Current treatments for the majority of cancers include surgery, chemotherapy, and radiotherapy.[2] However, 45% of cancer patients can be cured by surgery and only 5% can be cured by chemotherapy and radiotherapy.[2] Additionally, cancer radiotherapy requires optimization in terms of how to maximize cancer cell-killing capacity within an acceptable dose that adjacent healthy tissues can tolerate from radiation injury. Also, the administration of drugs during chemotherapy remains having difficulties since the lack of specificity and the poor drug accumulation in the tumors generate undesired side effects in healthy tissues.[3] Alternative solutions to face these challenges include targeted therapy and thermal ablation through the use of nanoparticles (NPs) such as gold NPs with anisotropic morphologies and magnetic NPs.[4] Because of this challenge in current cancer treatment, we have developed a nanostructured modular system with a high degree of hierarchy for the transport and release of drugs, and magneto- and photothermal treatment against cancer. The system consists of magnetic NPs (Fe_3O_4) in the core of a silica (SiO_2) shell and surrounded by multi-branched gold NPs (MBAuNPs). With each of these components, the system comprises superparamagnetic and magnetothermal behavior, hierarchical structure, and photothermal capacity. These properties were confirmed by Scanning (SEM) and Transmission Electron Microscopy (TEM), UV-Vis Spectroscopy, and the measurement of magnetic properties using a Physical Property Measurement System (PPMS). UV-Vis spectrum showed a broad absorbance that includes the near-infrared region (NIR), which makes it possible to use the system in photothermal therapy using radiation with the same wavelength, which is harmless to healthy tissues.[5] Also, SEM and TEM showed a core-shell system with optimal size and morphology (see Fig. 1). Finally, in terms of magnetic properties, the system showed a superparamagnetic behavior, which favors its use in biomedical applications since the NPs do not retain any remanent magnetization once the magnetic field is turned off.[6] In sum, cancer is a global disease with the highest mortality rate.[7] Traditional treatments such as surgery, chemotherapy, and radiotherapy have limited therapeutic effects against cancer and are associated with severe side effects, so they require optimization.[7] We report the development of a multifunctional nanostructured system for local magneto- and photothermal ablation and targeted drug delivery, with potential applications in the treatment of breast and cervical cancers. This purpose was achieved by synthesizing a modular system that is constituted by a magnetic core of Fe_3O_4 NPs, a protective layer of SiO_2, and MBAuNPs. The results imply that the optical, photothermal, and magnetic properties of this system are optimal for biomedical applications.

REFERENCES

[1] Sung H. et al. *CA: a cancer journal for clinicians* (2021) (71) (209-249)
[2] Chatterjee P. and Kumar S. *Materials Today.* (2022) (48) (1754-1758)
[3] Gonzalez-Valdivieso J. et al. *International Journal of Pharmaceutics* (2021) (599) (120438)
[4] Pucci C. et al. *Ecancermedicalscience* (2019) (13)
[5] Carreón-Álvarez C. *AIP Advances* (2020) (10) (125030)

[6] Hervault A. et al. Nanoscale (2014) (6) (11553–11573)
[7] Park W. et al. *Biomaterials research.* (2018) (22) (1-10)

ACKNOWLEDGMENTS

Verónica Quilumba-Dutan acknowledges M.C. Ana Iris Peña-Maldonado, Dr. Héctor Gabriel Silva-Pereyra, and M.C. Beatriz Adriana Rivera-Escoto for their helpful collaboration in the technical measurements using the SEM-EDS, HRTEM, and XRD infrastructure from LINAN-IPICYT. Also, the author appreciates the collaboration of Dr. José Luis Rodriguez-López for making available the laboratory of bio-nanostructures to meet the objectives of this research project. Likewise, the author appreciates all the work and guidance of Dr. Clara Carreón, Dr. Eugenia Valsami-Jones, Dr. Sergio Hidalgo, Dr. Rubén Lopez-Revilla, Dr. José Luis Rodriguez-López, and Dr. Swaroop Chakraborty. Finally, the author acknowledges the scholarship (1089707) offered by CONACYT for pursuing graduate studies.

FIGURES

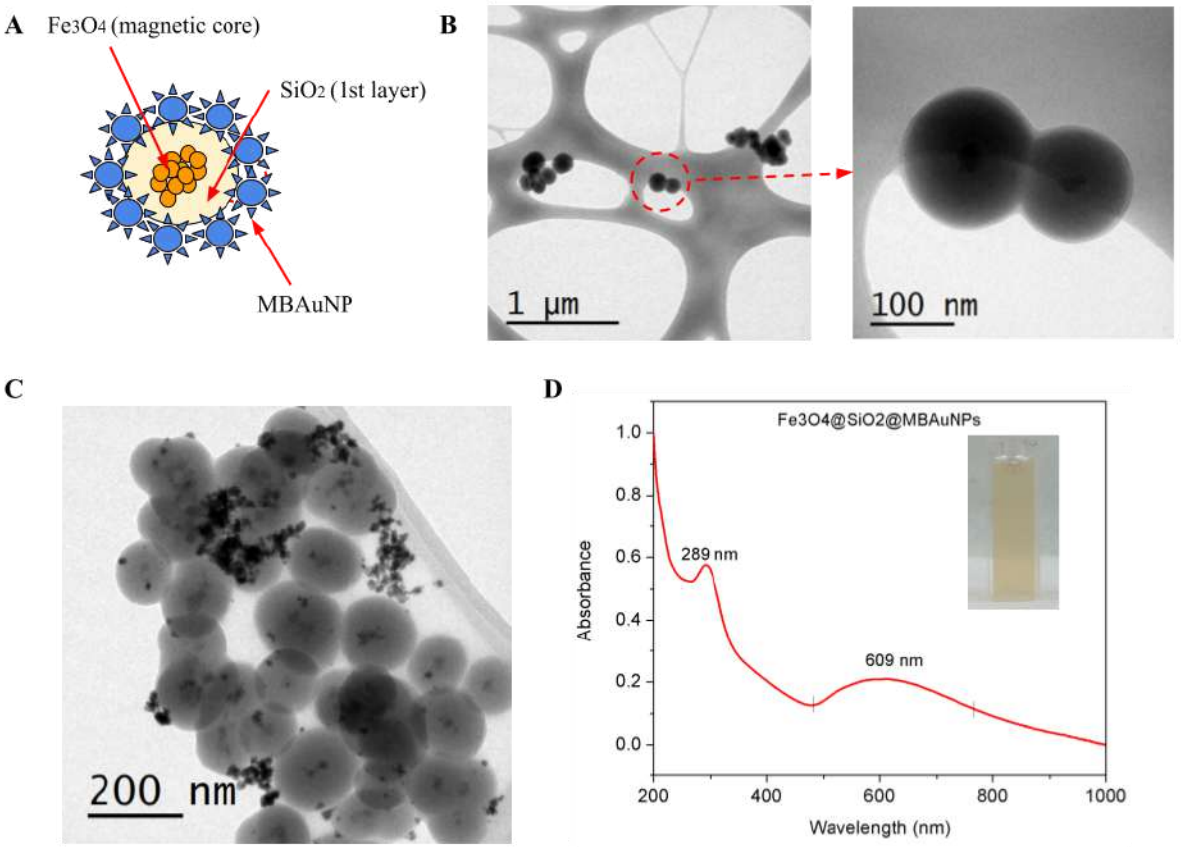

Figure. 1. A multifunctional nanostructured system. **A.** Hypothetical diagram of the modular Fe_3O_4@SiO_2@MBAuNPs system, with each of its components (Fe_3O_4 NPs, SiO_2, and MBAuNPs). **B.** TEM micrograph of core-shell NPs constituted by Fe_3O_4 NPs in the core of a SiO_2 layer. **C.** MBAuNPs surrounding the core-shell NPs in micrograph B. **D**. UV-Vis spectrum for the system Fe_3O_4@SiO_2@MBAuNPs with their maximum absorbance from the UV-Vis region to the NIR region.

Acta Microscopica Vol. 32, Supp. 1, 2023, pp. xx
PROCEEDINGS NSSY 2023- Galapagos 23th-29th April 2023

MECHANOCHEMICAL SYNTHESIS OF TANTALUM CARBIDE

Adriana Vázquez-Pelayo (1) and Miguel Avalos-Borja (1)

(1) División de Materiales Avanzados, Instituto Potosino de Investigación Científica y Tecnológica, San Luis Potosí, México.
adriana.vazquez@ipicyt.edu.mx

Research on new hard materials has been carried out to improve their characteristics and properties. Currently, materials of light elements and transition metals have gained interest, especially Transition Metal Carbides (TMC) [1]. Tantalum Carbide (TaC) is a promising compound for TMC, as it has very interesting characteristics and properties such as high hardness (17.54 GPa), high melting point (3880 °C) and resistance to chemical attack and oxidation [2]. However, these properties depend on synthesis method, crystalline structure, chemical bond, crystalline defects and grain size. Hot Pressing (HP), Hot Isostatic Processing (HIP) and Spark Plasma Sintering (SPS) are commonly used to consolidate TaC [3]. The aim of the present work was to synthesize TaC by using two very different techniques to improve hardness: mechanical milling (MM) and SPS. MM allows synthesizing materials under environmental conditions generating changes in the morphology and grain size that result in the improvement of hardness. SPS favors atomic diffusion and consolidates the samples at temperatures lower than melting point. Therefore, in this work, TaC was synthesized by MM from a stoichiometric powder mixture of tantalum and carbon with a 1:1 molar ratio. The formation of the material was obtained at 60 min milling time. X-ray diffraction, Scanning Electron Microscopy (SEM) and Transmission Electron Microscopy (TEM) were used to characterize the products. Subsequently, the samples were treated using SPS, reaching a maximum temperature of 1341 °C. Consolidated samples were characterized by X-ray diffraction and X-ray Photoelectron Spectroscopy (XPS) to determine changes in the crystalline structure of the material as well as elucidate the surface chemical composition of the samples. Microhardness was measured using Vickers indentation in accordance with ASTM Standard E384-17 by applying different loads (0.49, 0.98, 2.94, 4.9 and 9.8 N) with a dwell time of 15 s.

After MM, X-ray analysis shows the presence of Ta ($Im\bar{3}m$ space group), TaC ($Fm\bar{3}m$ space group) and WC ($P\bar{6}m2$ space group), WC comes from the milling material (bowl and balls). The morphology of the material is undefined and tends to form agglomerates with an average particle size of 1 µm. The diffraction patterns obtained are characteristic of a polycrystalline material and indicate the presence of TaC. HRTEM analysis shows interplanar distances 2.5 and 2.2 Å, corresponding to (111) and (200) TaC planes, as seen in the $[01\bar{1}]$ zone axis diffraction pattern. Simulations were carried out in the MacTempas software to corroborate the results obtained (see Figure 1).

After SPS treatment, a characterization of the sample was performed with X-ray diffraction and XPS techniques. X-ray diffraction analysis shows the presence of Ta_2O_5 (C2mm space group) which indicate the oxidation of the sample during the SPS, however there is no change in the other phases found in the material after MM. XPS analysis identifies TaC, WC and Ta_2O_5, corroborating the results obtained by X-ray diffraction, additionally, there is no indication of any contaminant on the sample surface. Vickers hardness test shows that hardness decreases as the load increases being a normal Indentation Size Effect (ISE). In the microhardness category with a load of 0.49 N, the sample has a Vickers hardness of 28.6±1.4 GPa, whilst at 0.98 N has a hardness of 23.1±0.9 GPa. On the other hand, within the low load category with an applied load of 4.9 N, the sample has a hardness of 18.2±0.5 GPa GPa and at 9.8 N a hardness of 17.6±0.8 GPa. Comparing the results obtained with other synthesis methods, the hardness in our samples is significantly higher than those reported in the literature (Table 1). Is important to mention that is the first time that TaC is synthesized by MM and afterwards treated by SPS.

REFERENCES

[1] Zhao Z. et al. Annu. Rev. Mater. Res. (2016).
[2] Jiang J. et al. Ceram. Int. (2016) (42) (7118).
[3] Nisar. et al. Int. J. Refract. Met. Hard Mater. (2018) (73) (221).

ACKNOWLEDGMENTS

AV-P acknowledges a scholarship granted by CONACyT. The authors thank LINAN-IPICyT and Polytechnique Montréal for the facilities provided and the access to laboratories. We also acknowledge technical support provided by Beatriz Rivera in X-rays diffraction, Ignacio Becerril in SEM and Vickers hardness test, Jean Philippe Masse in TEM and Josianne Lefebvre in XPS.

FIGURES

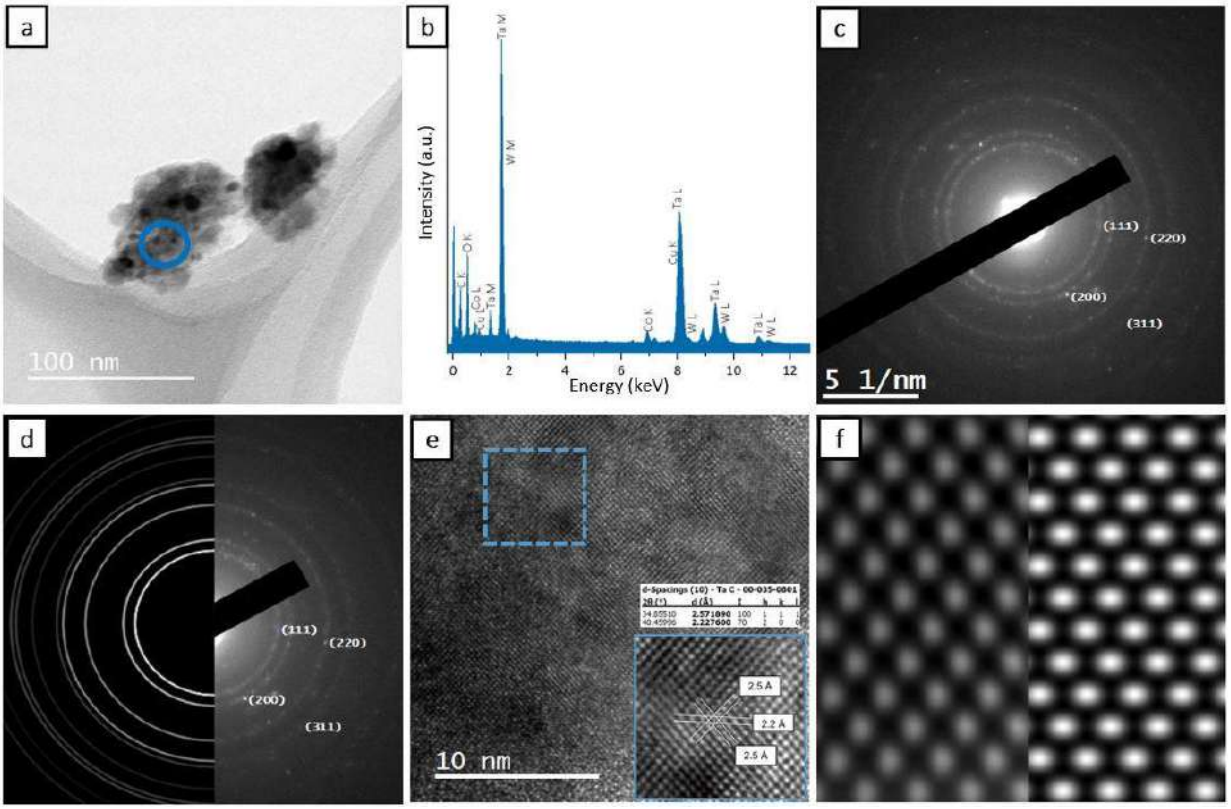

Figure 1. TEM micrographs, a) low magnification, b) EDS from the blue area in a), c) electron diffraction pattern, d) simulated vs experimental DP, e) HRTEM, and f) experimental HRTEM vs simulated.

Table 1. Comparison of Vickers hardness obtained in the present work vs reported in the literature.

Reference	Applied load 9.8 N	Applied load 4.9 N	Applied load 0.49 N
Present work	17.6±0.8 GPa	18.2±0.5 GPa	28.6±1.4 GPa
Cedillos-Barraza et al.	13.9±0.7, 20.4±2.3 GPa		
Silvestroni et al.	11.1±0.7, 13.7±0.3 GPa		
Zhang et al.		14.1±0.2, 16.3±0.2 GPa	
Srinivasa et al.		17.8±3.2, 24.6±2.2 GPa	
Zhao et al.			18.6±0.9 GPa
Weiguo et al.		21.9±0.6 GPa	28.2±0.7 GPa

THURSDAY

Synthesis of Nanostructures

Acta Microscopica Vol. 32, Supp. 1, 2023, pp. xx
PROCEEDINGS NSSY 2023- Galapagos 23th-29th April 2023

NANOSTRUCTURED SURFACES AS AN INTERESTING ALTERNATIVE FOR ACHIEVING SDG 6 ELECTROCHEMICAL-BASED SOLUTIONS

Karla C. de Freitas Araújo (1), Luis D. Loor-Urgilés (1), Pollyana Castro (1), Amanda D. Gondim (1), Lívia N. Cavalcanti (1), Elisama V. dos Santos (1), Mattia Pierpaoli (2), Mateusz Ficek (2), José Eudes L. Santos (1), Robert Bogdanowicz (2), Carlos A. Martínez-Huitle (1)

(1) Renewable Energies and Environmental Sustainability Research Group, Institute of Chemistry, Federal University of Rio Grande do Norte, Campus Universitário, Av. Salgado Filho 3000, Lagoa Nova, CEP 59078-970, Natal, Rio Grande do Norte, Brazil (2) Faculty of Electronics, Telecommunications and Informatics, Gdańsk University of Technology, 11/12 G. Narutowicza St, Gdańsk 80-233, Poland.
carlosmh@quimica.ufrn.br

In order to create a better and more sustainable future for all societies worldwide, the United Nations Member States have created the Sustainable Development Goals (SDGs). 17 SDGs were established in several subject areas, such as water, energy, climate, oceans, urbanization, transport, science, and technology, to achieve this. Materials science has considerably contributed to the accomplishment of several SDGs, according to report maps of the most current sustainability initiatives and research within each SDG area [3,4]. Advanced materials, for instance, may aid in achieving development objectives in key areas of focus on zero hunger (SDG 2), good health and well-being (SDG 3), clean water and sanitation (SDG 6), affordable and clean energy (SDG 7), industry, innovation and infrastructure (SDG 9), sustainable cities and communities (SDG 11), responsible consumption and production (SDG 12), climate action (SDG 13), and life below water (SDG 14). Then, the scientific and technological domains may develop and construct practical solutions in materials and their applications by identifying essential insights to open novel branches and landscapes for maximizing social benefits. Within this framework, innovative approaches to catalyst creation and electrode production are explored by electrochemistry, electrochemical engineering and material sciences in themes that aim to increase environmental sustainability.

To increase the synergistic effects of electrocatalytic materials to produce potent oxidant species or to increase the active sites on their surfaces, as well as to improve the conversion yield in a fuel cell, high-added-value products, electrolytic treatment for environmental protection, or the detection limit in electroanalysis, the introduction of nanotechnology appears to be a crucial factor. Recently, using the microwave plasma-assisted chemical vapor deposition (CVD) procedure, a novel type of 3D-diamond electrodes with boron-doped carbon nanowalls (B:CNW) was recently produced (Fig. 1), increasing charge transfer and boosting electrochemical performance (Fig. 1a). The usefulness of a boron doped diamond/boron-doped carbon nanowalls (BDD/B:CNW) anodes to degrade organic pollutants has been already examined; however, no efforts at the electrosynthesis of oxidizing species utilizing these diamond-carbon nanostructures have been documented yet. Consequently, the electrosynthesis of sulfate-based oxidizing species was investigated here to provide pertinent answers from both a theoretical and practical standpoint. In the case of electrogenerated oxidizing species, the advances on the identification strategies have facilitated to understand the effect of different experimental factors on their production as well as to comprehend the reactions promoted by them, close to the electrode surface or in the bulk. The majority of EAOPs are based on the production of heterogeneous or homogeneous hydroxyl radicals (•OH) in water medium, and in turn, the modifications in the electrochemical systems to enhance its production, for example, by changing the nature of electrodes (active and nonactive) or by exciting the system with ultrasounds or light irradiation. However, the oxidation via heterogeneous or homogeneous •OH has some advantages and disadvantages. Typically, it quickly occurs as a surface-layer phenomenon inside the reaction cage (i.e. Nernst layer and close to it) with heterogeneous •OH or as volume-oxidation approach in the bulk with homogeneous •OH, due to their concentration and extinction time. For this reason, other oxidants, such as persulfate ($S_2O_8^{2-}$) and sulfate radical ($SO_4^{\bullet-}$), have recently received great attention by the scientific community because of their advantages over •OH, for example, lifetime is more substantial. Persulfate is a relatively stable oxidizing agent that can be electrochemically produced at high concentrations, from the EO of sulfate species see Fig. 1e), depending on the kind of electrode (its formation has been only confirmed at

Pt, doped, and suboxides of Ti, Pb-based oxides, as well as diamond electrodes), electrolyte medium, and its concentration used as well as the current or potential applied. Diamond films are one of the most efficient and inert electrodes for the electrogeneration of $S_2O_8^{2-}$ considering that: (i) $S_2O_8^{2-}$ formation, from the EO of sulfate species, depends on the properties of the electrode (boron doping, sp^2/sp^3 ratio, roughness, electrode support, and thickness), electrolyte medium (sulfuric acid, sulfuric-based acids, or sulfate salts) and its concentration (from 0.1 to 1 mol L^{-1}), as well as the organic-sulfate salt precursor; and (ii) direct ($2SO_4^{2-} \rightarrow S_2O_8^{2-} + 2e^-$, see Fig. 1) or indirect mechanisms are the main routes to electrogenerate $S_2O_8^{2-}$ at diamond films. But, considering that $SO_4^{\bullet-}$ can be generated via reaction with heterogeneous free $^{\bullet}OH$ ($SO_4^{2-} + {}^{\bullet}OH \rightarrow \rightarrow 2SO_4^{\bullet-} \rightarrow S_2O_8^{2-}$), which is formed via water discharge (BDD + $H_2O \rightarrow$ BDD($^{\bullet}OH$) + $H^+ + e^-$, Fig. 1), at indirect mechanism.

In this study, the results revealed that persulfate was easily formed at the BBD electrode, whereas that the ion-radical sulfate might be the most important oxidant at BDD/B:CNW anode when the electrogeneration was compared to other electrocatalytic materials, including BDD surfaces (Fig. 1b). At diamond electrodes, persulfate concentrations varied between 3 and 6 M according to the applied current density (2.5, 5.0, and 15 mA cm^2). Using BDD/B:CNW, methyl orange (MO), a dye-model pollutant, was broken down below the limit of detection in 45 minutes when in-situ sulfate-based oxidizing species were electrogenerated. Residual organic matter in solution, in terms of chemical oxygen demand (COD) values (Fig. 1d), as a function of applied current density (2.5 and 15.0 mA cm^{-2}), after 40 min of electrolysis at different anodic materials in electrochemical oxidation tests at 25 °C showed that BDD/B:CNW anode was an efficient electrocatalytic material, depolluting the synthetic effluent via the action of $S_2O_8^{2-}$ and $SO_4^{\bullet-}$. As innovative electrocatalysts for diverse catalytic applications in the environmental and energy domains, these forms of 3D diamond-carbon nanostructures are therefore promising. In summary, we can conclude that, (i) BDD/B:CNW electrode is constituted by 3D-diamond-carbon nanostructures which increase significantly its electroactive surface area, (ii) in diamond materials, electrochemical measurements have indicated that the complex set of the electrochemical reactions takes at lower and higher over potential regions. However, it mainly seems that the persulfate electrosynthesis depends on the stability/reactivity of $^{\bullet}OH$ and diamond surface active sites to favor the production of SO4−·. In the case of BDD/B:CNW electrode, $SO_4^{\bullet-}$ species are adsorbed at sp^2-active sites, favoring their participation in the oxidation of MO.

REFERENCES

[1] Martínez-Huitle, C.A. et al. *Appl Catal B* (2023) (328) (122430).
[2] de Freitas Araújo, K.C. et al. *Electrochim Acta* (2022) (430) (141069).

ACKNOWLEDGMENTS

Financial support from Conselho Nacional de Desenvolvimento Científico e Tecnológico (CNPq, Brazil) (306323/2018-4, 312595/2019-0, 439344/2018-2, 315879/2021-1, 409196/2022-3, 408110/2022-8), and from Fundação de Amparo à Pesquisa do Estado de São Paulo (Brazil), FAPESP 2014/50945-4 and 2019/13113-4, are gratefully acknowledged.

FIGURES

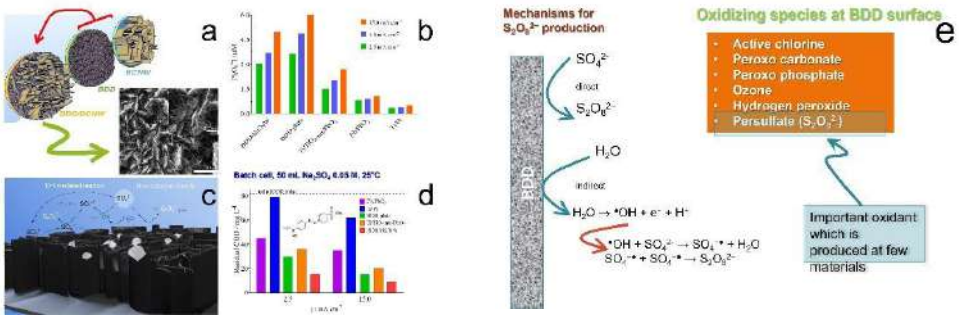

Figure 1. (a) BDD/B:CNW electrode morphology, as observed in the SEM images, (b) production of persulfate at different electrode materials, (c) $S_2O_8^{2-}$ and $SO_4^{\bullet-}$ mechanisms at BDD/B:CNW, (d) COD removal at 2.5 and 15 mA cm^2, (e) persulfate mechanisms electrogeneration.

Acta Microscopica Vol. 32, Supp. 1, 2023, pp. xx
PROCEEDINGS NSSY 2023- Galapagos 23th-29th April 2023

PURE WATER: THINKING SUSTAINABLY TO REMOVE TOXIC AND RECALCITRANT POLLUTANTS USING NANOPARTICLES AND NANOCOMPOSITES

Víctor H. Guerrero (1), Jennifer Tejedor (1), Carla Valdivieso Ramirez (1)

(1) Department of Materials, Escuela Politécnica Nacional, Quito 170525, Ecuador.
victor.guerrero@epn.edu.ec

Besides impressive social and technological innovations, the last century brought a continuous increase in the population, especially rapid in several developing and emerging countries. This has been associated with growing water, food and energy demands. In particular, the increase in the global demand for clean water and the decrease in the availability of natural renewable resources results in a deteriorating water quality and high pressures on water resources. This, combined with the impacts of phenomena such as climate change and contamination, may have a tremendous effect on agriculture and food supply, health problems, energy markets, and potential for conflicts, among others [1]. Considering these perspectives, it is of paramount importance to develop materials, processes and technologies that could help removing contaminants from water. In this work, the use of nanoparticles and nanocomposites was evaluated, focusing on those that can be synthesized in an environmentally friendly manner, and that can be used to eliminate synthetic dyes, toxic and recalcitrant organic pollutants, and heavy metals. For this purpose, iron oxide and silicon oxide nanoparticles were synthesized using traditional methods, to be compared to eco-friendly approaches employing fruits extracts and organic acids. The nanocomposites were obtained by impregnating the nanoparticles on low-cost, abundant, highly available and easy-to-process agroindustrial lignocellulosic residues. Additionally, graphene oxide (GO) was synthesized following a modified Marcano method, and used to obtain nanocomposites. Characterization techniques such as X-ray diffraction (XRD), scanning (SEM) and transmission (TEM) electron microscopies, dynamic light scattering (DLS), Fourier transform infrared (FTIR), UV-Vis and Raman spectroscopies, and nitrogen adsorption were used to analyze the materials obtained. These analyses allowed to determine the composition, structure, size, surface morphology and functionality, as well as the specific surface area and porosity of the materials obtained. XRD showed that the iron oxide particles were, in general, composed of mixtures of magnetite (Fe_3O_4), hematite (α-Fe_2O_3) and maghemite (γ-Fe_2O_3); while the silica particles were composed of SiO_2. The TEM and DLS analyses confirmed the formation of spherical nanoparticles with sizes ranging from about 5 to 30 nm for the iron oxide, and between about 5 and 10 nm for the silica. FTIR analyses showed that the lignocellulosic residues exhibited mostly hydroxyl and carboxyl groups, which could interact with contaminants and favor their removal from aqueous solutions [2]. Raman spectroscopy analyses performed on the GO exhibited the characteristic D, G and 2D bands, with a I_D/I_G ratio of 0.88, which was greater than that for the graphite (0.43) used as precursor [3]. The specific surface area obtained using the Brunauer-Emmett-Teller method showed values up to about 60, 220, and 260 m^2/g for iron oxide, silica and GO, respectively. The lignocellulosic residues had specific surface areas of the order of 1 m^2/g. Batch test analyses demonstrated that the nanoparticles synthesized using agricultural residues, as extracts or as precursors, showed high adsorption performance for removing dyes (e.g., methylene blue and methyl orange), emerging contaminants (e.g., caffeine, triclosan), and heavy metal ions (e.g., Zn(II), Cr(VI)). It is worth mentioning that the iron oxide nanoparticles also exhibited antioxidant activities against 1,1-diphenyl-2-picrylhydrazyl (DPPH). The lignocellulosic residues (e.g., fruit peels, sawdust) showed also high removal efficiencies but relatively low adsorptive capacities. The addition of nanoparticles to these residues improved the adsorptive capacities and efficiencies, and reduced the optimal contact times for the composites. The adsorption data fitted well, in general, the Freundlich and Sips isotherm models, as well as the pseudo-second-order kinetics model. Summarizing, the results obtained indicate that agricultural residues offer low-cost, sustainable alternatives to synthetize high performance adsorbents. They also allow us to define strategies and select materials that could be advantageously integrated in water treatment technologies.

Acta Microscopica Vol. 32, Supp. 1, 2023, pp. xx
PROCEEDINGS NSSY 2023- Galapagos 23th-29th April 2023

REFERENCES

[1] Borgomeo E. et al. *Earth's Future* (2020) (8) (e2020EF001495).
[2] Stjepanovic M. et al. *J. Mol. Liq.* (2019) (285) (535).
[3] Almeida-Naranjo C. (2023) *Remediation* (2023).

ACKNOWLEDGMENTS

The authors would like to acknowledge the support of the Escuela Politécnica Nacional through the project grants PIS-18-01, PIGR-19-05, and PIM-20-03.

Acta Microscopica Vol. 32, Supp. 1, 2023, pp. xx
PROCEEDINGS NSSY 2023- Galapagos 23th-29th April 2023

CITOTOXICITY OF NANOPARTICLES WITH BIOMEDICAL APPLICATIONS AN OVERVIEW

Lenin J. Ramírez-Cando (1), Nayeli Gómez (1), Raúl Davalos-Monteiro (1), Carlos Reinoso (2), and, Ronny Ordoñez (1)

(1) School of Biological Sciences and Engineering, Yachay University for Experimental Technology and Research (Yachay Tech), Hacienda San José S/N, Proyecto Yachay, 100115, Urcuquí, Ecuador.
(2) School of Physical Sciences and Nanotechnology, Yachay University for Experimental Technology and Research (Yachay Tech), Hacienda San José S/N, Proyecto Yachay, 100115, Urcuquí, Ecuador.
lramirez@yachaytech.edu.ec

Recently there has been a great interest in nanoparticles (NPs) as potential therapeutic agents. The shortcomings of conventional non-biological synthesis methods such as generation of toxic byproducts, energy consumptions, and involved cost have shifted the attention towards green syntheses of NPs. Among noble metal NPs, gold nanoparticles (AuNPs), silver (AgNPs) and iron oxides IONPs are the most extensively used ones, owing to their unique physicochemical properties. NPs have potential therapeutic applications, as those are synthesized with biomolecules as reducing and stabilizing agent(s). The new methods of NPs synthesis are simple, eco-friendly, and cost-effective with the use of renewable energy sources, despite this their toxicity is not well-known yet. Although thousands of different nanoparticles (NPs) have been identified and synthesized to date, well-defined, consistent guidelines to control their exposure and evaluate their potential toxicity have yet to be fully established. As potential applications of nanotechnology in numerous fields multiply, there is an increased awareness of the issue of nanomaterials' toxicity among scientists and producers managing them. An updated inventory of customer products containing NPs estimates that they currently number over 5.000; ten years ago, they were one fifth of this. More often than not, products bear no information regarding the presence of NPs in the indicated list of ingredients or components. Consumers are therefore largely unaware of the extent to which nanomaterials have entered our lives, let alone their potential risks. Moreover, the lack of certainties with regard to the safe use of NPs is curbing their applications in the biomedical field, especially in the diagnosis and treatment of cancer, where they are performing outstandingly but are not yet being exploited as much as they could. The production of radical oxygen species is a predominant mechanism leading to metal NPs-driven carcinogenesis. The release of particularly reactive metal ions capable of crossing cell membranes has also been implicated in NPs toxicity. In this overview we discuss the origin, behavior and biological toxicity of different metal NPs with the aim of rationalizing related health hazards and calling attention to toxicological concerns involved in their increasingly widespread use.

Acta Microscopica Vol. 32, Supp. 1, 2023, pp. xx
PROCEEDINGS NSSY 2023- Galapagos 23th-29th April 2023

CONVERTING POLYMERIC SOLUTIONS INTO BIOMEDICAL NANOFIBERS THROUGH ELECTROSPINNING - AN OVERVIEW OF WORKING PARAMETERS

E. Chuisaca-Londa [a], D. Osorio-Ordóñez [a], J. Dávalos-Monteiro [b], L. Ramirez-Cando [a], R. Dávalos-Monteiro [a, c] *

[a] School of Biological Science and Engineering, Yachay Tech University, Urcuquí, Ecuador.
[a] King Abdullah University of Science and Technology KAUST, Thuwal, Kingdom of Saudi Arabia.
[c] Advanced Materials Research Group (GIMA) - Superior Polytechnical School of Chimborazo, Riobamba, Ecuador.
rdavalos@yachaytech.edu.ec

Electrospinning is perhaps the most flexible method to produce nanofibers nowadays. Polymeric solutions are capable of being converted into nanofibers with a wide variety of biomedical applications, from wound healing textiles to smart and complex drug delivery systems. The production of these biomedical nanofibers depends on the correct application of the working parameters. The analysis of the electrospinning working parameters are divided into three main streams: i) the electrospinning equipment conditions, ii) the polymeric solution properties and iii) the ambient conditions. In this work, a detailed overview of the electrospinning working parameters and their impact in the final production of biomedical nanofibers is presented.

REFERENCES

[1] Teo, W. E., & Ramakrishna, S. (2006). A review on electrospinning design and nanofibre assemblies. Nanotechnology, 17(14), R89.

[2] Agarwal, S., Wendorff, J. H., & Greiner, A. (2008). Use of electrospinning technique for biomedical applications. Polymer, 49(26), 5603-5621.

[3] Poshina, D., & Otsuka, I. (2021). Electrospun Polysaccharidic Textiles for Biomedical Applications. Textiles, 1(2), 152-169.

[4] Sinha, M. K., Das, B. R., Bharathi, D., Prasad, N. E., Kishore, B., Raj, P., & Kumar, K. (2020). Electrospun nanofibrous materials for biomedical textiles. Materials Today: Proceedings, 21, 1818-1826.

[5] Kailasa, S., Reddy, M. S. B., Maurya, M. R., Rani, B. G., Rao, K. V., & Sadasivuni, K. K. (2021). Electrospun nanofibers: materials, synthesis parameters, and their role in sensing applications. Macromolecular Materials and Engineering, 306(11), 2100410.

[6] Chen, S., Li, R., Li, X., & Xie, J. (2018). Electrospinning: An enabling nanotechnology platform for drug delivery and regenerative medicine. Advanced drug delivery reviews, 132, 188-213.

[7] Cseri, L., Topuz, F., Abdulhamid, M. A., Alammar, A., Budd, P. M., & Szekely, G. (2021). Electrospun adsorptive nanofibrous membranes from ion exchange polymers to snare textile dyes from wastewater. Advanced Materials Technologies, 6(10), 2000955.

[8] Sun, G., Sun, L., Xie, H., & Liu, J. (2016). Electrospinning of nanofibers for energy applications. Nanomaterials, 6(7), 129.

[9] Villarreal-Gómez, L. J., Cornejo-Bravo, J. M., Vera-Graziano, R., & Grande, D. (2016). Electrospinning as a powerful technique for biomedical applications: a critically selected survey. Journal of biomaterials science, polymer edition, 27(2), 157-176.

[10] Meinel, A. J., Germershaus, O., Luhmann, T., Merkle, H. P., & Meinel, L. (2012). Electrospun matrices for localized drug delivery: current technologies and selected biomedical applications. European Journal of Pharmaceutics and Biopharmaceutics, 81(1), 1-13.

[11] Cheng, H., Yang, X., Che, X., Yang, M., & Zhai, G. (2018). Biomedical application and controlled drug release of electrospun fibrous materials. Materials Science and Engineering: C, 90, 750-763.

[12] T. Mazoochi, V. Jabbari (2011), Chitosan nanofibrous scaffold fabricated via electrospinning: the effect of processing parameters on the nanofiber morphology, Int. J. Polym. Anal. Char. 16 277–289.

[13] Taylor G (1964) Disintegration of water drops in an electric feld. Proc R Soc Lond A 280(1382):383–397

[14] Haider, A., Haider, S., & Kang, I.-K. (2015). A comprehensive review summarizing the effect of electrospinning parameters and potential applications of nanofibers in biomedical and biotechnology. Arabian Journal of Chemistry. doi:10.1016/j.arabjc.2015.11.015

[15] Hu, J.; Wang, X.; Ding, B.; Lin, J.; Yu, J.; Sun, G. (2011). One-Step Electro-Spinning/Netting Technique for Controllably Preparing Polyurethane Nano-Fiber/Net. Macromol. Rapid Commun., 32, 1729−1734.

[16] Ibrahim, H.M., & Klingner, A. (2020). A review on electrospun polymeric nanofibers: Production parameters and potential applications. Polymer Testing, 90, 106647.

ACKNOWLEDGMENTS

Authors want to thank the Biomaterials Laboratory of the School of Biological Sciences and Engineering at Yachay Tech University for supporting this research project.

FIGURES

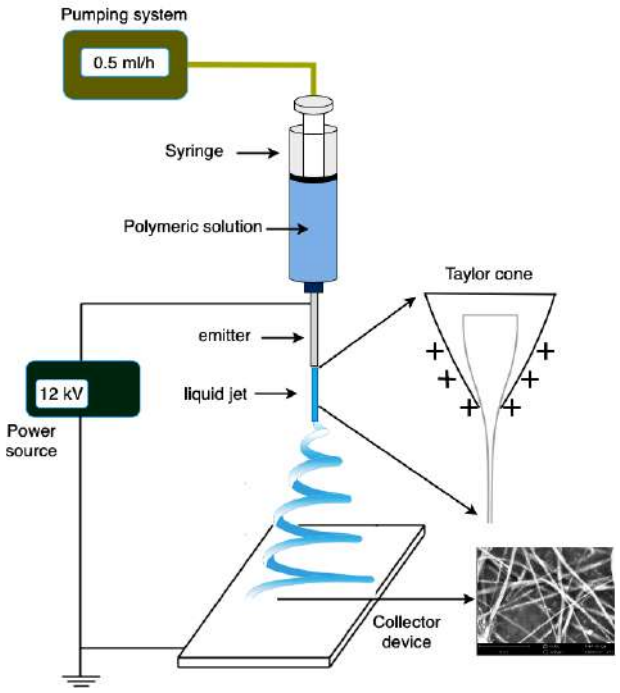

Figure 1. Electrospinning Schematic for nanofiber production

Acta Microscopica Vol. 32, Supp. 1, 2023, pp. xx
PROCEEDINGS NSSY 2023- Galapagos 23th-29th April 2023

SILVER NANOPARTICLES AND ITS APLICATION IN PRESERVATIVE SOLUTIONS OF CUT FLOWERS

Hilda-Araceli Zavaleta-Mancera (1), Itzel Villegas-Velázquez (1), Columba Vicencio-Salas Solís (2), Luis Manuel Carrillo-López (3).

(1) Botany Department, Colegio de Postgraduados en Ciencias Agrícolas (COLPOS), Montecillo, Texcoco México. (2) Plant Physiology Department, COLPOS (3) Faculty of Zootechnics and Ecology, CONACYT-Universidad Autónoma de Chihuahua, Mexico.
arazavaleta@colpos.mx

Silver nanoparticles (AgNPs) are well recognized by its antibacterial properties because they reduce cytoplasmic membrane thickness, lose the cell wall, and condense DNA molecules. Floriculture is an intensive type of agriculture and the income per unit area from floriculture is much higher than any other branch of agriculture. Cut flowers are very important for human society: they offer beauty and spirit comfort, they offer sick's to speed recovery, they are used to express love, happiness, in birthdays or gratefulness worship in temples. In Mexico, cut flowers are a big industry, 20% of our production is exported to the USA and Canada, but the losses at postharvest carry significant economic losses because of poor management, attack by microorganisms, and vascular system blockage from bacteria and embolism (bubble airs). Ag^{+} are known to be a good antibacterial agent and prevent ethylene ($H_2C=CH_2$) production, the hormone of plant senescence. The objective of the present research was comparing the capacity of biosynthesized AgNPs to extend vase life of Chrysanthemum, Roses and Alstroemeria, which are some of the most commercialized flowers in Mexico and in the world. For *Chrysanthemum* experiments we used AgNps synthesized with 5 mL of *Chemopodium abrosioides* extracts and 10 mM $AgNO_3$ according to López-Carrillo et al. (2014). For Roses and Alstroemeria experiments we used AgNps synthesized with 3 mL *Camelia sinensis* extract according to Nakhjavani, M. et al. (2017). Flowers were obtained from Coxflor company and local growers from the Estate of México. For all experiments the design was completely random with 5-15 replicas. For *Chrysanthemum* cv. Puma, AgNps (10.2 ± 4.3 nm) (0.01, 0.05, 0.1, 0.5, 1.0 mM) were added to the preservative solution: vase life and bacterial counting was compared to control (Fig. 1). Low concentrations (0.01, 0.05 mM) of AgNPs increased vase life, promoted inflorescence diameter, and reduce bacterial count (Table 1). For *Rosa hybrid* cv. Freedom, we use AgNPs of 21.50 ±0.63 (Fig. 2). The treatments were: a) 1.0 mg L^{-1} AgNPs, b) 1.0 mg L-1 AgNPs + 2% sucrose, c) 1.0 mg L^{-1} AgNPs + 80 mgL^{-1} citric acid, pH 4, d) 1.0 mg L^{-1} AgNPs + 2% sucrose + citric acid, e) control (water). Ag NPs + citric acid had the longest vase life, large consumption (147.08 mL) and reduction of bacterial population (Table 2). It has been reported the beneficial effects of sucrose in preservative solutions but in Rose it increased bacterial counting. For *Alstroemeria* cv. Fogo we use AgNPs of 15.79 nm diameter and 0.85 roundness (Fig. 3). We screened AgNps (0, 4, 8, 16, 32, 50, 66, 94, 132 mg L^{-1} NPsAg) to pulse solution but it did not increase vase life. Combination of pulse solution (50 mg L^{-1}) and vase solution (0.5 mg L^{-1} NPsAg) was tested: a) pulsing for 24 h, b) pulsing + preservative solution, c) spraying pulse solution, and d) control (water).). When NPsAg was added to the preservative solution, antimicrobial activity was observed but no positive effect on vase life. We arrived at the conclusion that the vase life response was related to the degree of ethylene sensitivity of each specie. *Alstroemeria*, is a flower reported as low/not sensitive to ethylene y contrast *Rosa hybrida* respond to AgNPs because most of the cultivars are high ethylene sensitive. *Chrysanthemum*, is reported as a medium ethylene sensitive flower. But in all cases bacteria contamination was controlled by the AgNPs, it is a very desirable effect for postharvest management and flower exportation.

REFERENCES

[1] Nakhjavani, M. et al. 2017. *Heat Mass Transfer.* (2017) (53):3201-3209. Doi:10.1007/s00231-017-2065-9
[2] Carrillo- López L.M. et al., *J. Nanomaterials*. (2016) (Doi:10.1155/2016/951750)
[3] Vicencio-Salas Solís C. et al., *Agrociencia* (2018) (52):951-965.

ACKNOWLEDGMENTS

The authors thank CONACyT for the Master and PhD scholarships of the second and third authors. We are grateful to Simon Morales for technical assistance at the Electron Microscopy Unit of the Postgraduate Collage of Agriculture (UME-CP).

FIGURES

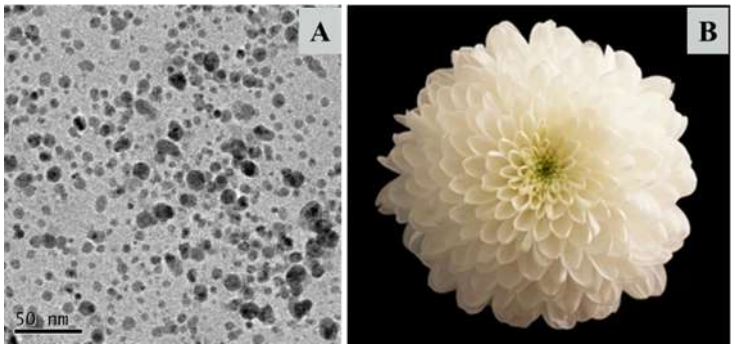

Figure. 1 Silver nanoparticles and plant material. A. Electron micrograph of AgNPs (10.2 ± 4.3 nm, 0.87 roundeness) synthesized with *C. abrosioides* extracts, TEM (Tecnai Spirit 2, Thermo Fisher) 100 keV and B. *Chrysanthemum* cv. Puma at harvest.

Table 1. Effect of Ag nanoparticle concentration (mM) on vase life (d), opening of *Chrysanthemum* inflorescences and bacterial inhibition in preservative solution.

AgNps (mM)	Vase life (d)	Diameter Inflorescences (cm)	Bacterial count (UCFmL^{-1})
control	12b	6.23c	105
0.01	21a	6.86b	2c
0.5	19.33a	6.96a	1c
0.10	19.33a	7.03a	0c
0.50	17.33b	6.16b	0c
1.0	17.00b	5.83b	0c
5.0	15.66b	6.16b	102c

Bacterial count is average of 5 experiments. Different letters in columns indicate statistical differences (Tuckey $p<0.05$)

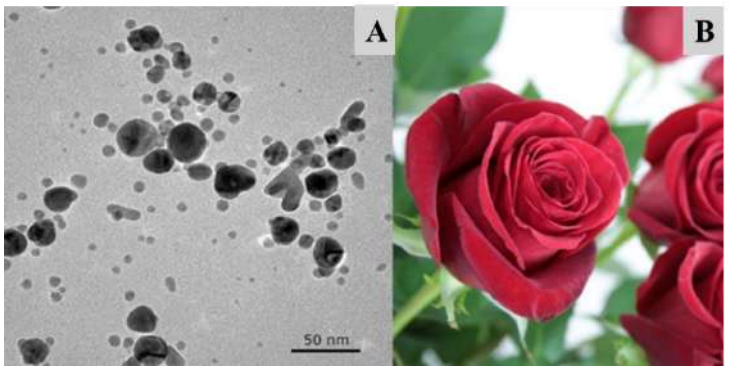

Figure. 2 Silver nanoparticles and plant material. A. Electron micrograph of AgNPs (21.50 nm, 0.86 roundness) synthesized with *C. sinensis* extracts, TEM (Tecnai Spirit 2, Thermo Fisher) 100 keV, B. *Rosa hybrid* cv. Fredom at harvest.

Table 2. Effect of AgNPs treatments on vase life, accumulated water consumption of *Rosa hybrida* cv. Fredom and bacterial count preservative solution (day 8).

AgNPs treatments	Vase life (d)	Water Consumption (mL)	Bacterial count (UCFmL^{-1})
Control	3.2c	96.8c	3.51a
NPs	5.4b	126.40b	2.36ab
NPs+S	3.9c	86.29d	2.91a
NPs+CA	7.5 a	147.08a	0.85a
NPs+CA+S	5.3 b	116.86b	1.26b

CA: 80 mgL^{-1}, Citric acid, S: 2% sucrose. Different letters in columns indicate significant differences (Tukey, $p<0.05$, n=15)

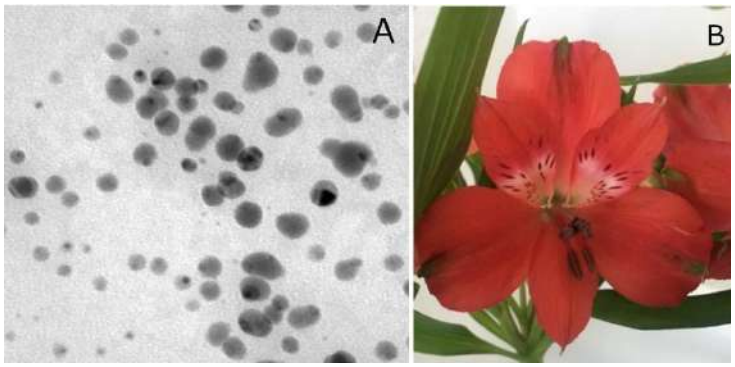

Figure. 2 Silver nanoparticles and plant material. A. Electron micrograph of AgNPs (15.79 nm, 0.85 roundness) synthesized with *C. sinensis* extracts, TEM (Tecnai Spirit 2, Thermo Fisher)100 keV, B. *Alstroemeria* cv. Fogo at harvest.

Table 3. Effect of AgNPs treatments on vase life, relative fresh weight (%) and Total chlorophyll (µg cm^{-2}) at final vase life of *Alsroemeria* cv. Fogo at harvest (day 21).

AgNPs Treatments (mgL^{-1})	Relative fresh weight (%)	Total Chl (µg cm^{-2})
Control	76.70	20.08
Pulse *	84.87	26.79
Pulse*+preservative**	85.96	25.09
Spraying *	86.48	13.39

(*) AgNPs 50 mgL^{-1}, (**) AgNPs 0.5 mg L^{-1}. No significant differences in columns (Tukey, $p<0.05$, n=15).

Acta Microscopica Vol. 32, Supp. 1, 2023, pp. xx
PROCEEDINGS NSSY 2023- Galapagos 23th-29th April 2023

RAMAN SPECTROSCOPY: INNOVATIVE SAMPLE SCANNING METHODS, ARTIFICIAL INTELLIGENCE CHEMOMETRICS, IMAGE MICROGEOPROCESSING AND COLOCALIZED MEASUREMENTS WITH SCANNING ELECTRON MICROSCOPY AND X-RAY MICROFLUORESCENCE.

Igor Carvalho (1), Filipe Cabral (1)
(1) Horiba Scientific Brazil, Jundiai – São Paulo, Brazil.
igor.carvalho@horiba.com

This presentation will focus on Raman and NanoRaman applied to the most diverse branches of knowledge. In this presentation you will learn the basic principles of Raman spectroscopy applied to Raman imaging. Applications and instrumentation will be the main topics for a wide range of materials characterization, including polymers, ceramics, biomaterials, life sciences and two-dimensional (2D) materials. Raman and Nanoraman microscopy is one of the only techniques capable of providing non-destructive, accurate analysis combined with high resolution images. Raman spectroscopy provides valuable information about the studied sample, such as chemical and structural composition. Based on the light-matter interaction, we obtain relevant information, such as: particle distribution, homogeneity, grain size, phase changes and several other characteristics of the sample through the chemical evaluation of the material. We will also discuss the combination of laser-excited photoluminescence imaging and Raman scattering of two-dimensional (2D) crystals to reveal the solid-state structure. The development of instrumentation makes possible the hyphenation of Raman with other techniques, such as Photoluminescence and AFM, being able to reach resolutions on a nanometric scale. The technique can be applied in several areas of knowledge, such as pharmaceuticals, photovoltaics, graphene, cells, nanoparticles, microplastics, among others.

Acta Microscopica Vol. 32, Supp. 1, 2023, pp. xx
PROCEEDINGS NSSY 2023- Galapagos 23th-29th April 2023

ANISOTROPIC VORTEX SQUEEZING AND SUPERCURRENT DIODE EFFECT IN NON-CENTROSYMMETRIC RASHBA SUPERCONDUCTORS

D. Kochan1,2

1 Institute for Theoretical Physics, University of Regensburg, 93040 Regensburg, Germany
2 Institute of Physics, Slovak Academy of Sciences, 84511 Bratislava, Slovakia
denis.kochan@ur.de

Most of 2D superconductors are of type II, i.e., they are penetrated by quantized vortices when exposed to out-of-plane magnetic fields. In the presence of a supercurrent, a Lorentz-like force acts on the vortices, leading to drift and dissipation. The current-induced vortex motion is impeded by pinning at defects. Usually, the pinning strength decreases upon any type of pair-breaking interaction that perturbs a system.
In the talk I will discuss surprising experimental evidence showing an unexpected enhancement of pinning in synthetic Rashba 2D superconductors when applying an in-plane magnetic field. When rotating the in-plane component of the field with respect to the driving current, the vortex inductance turns out to be highly anisotropic. We explain this phenomenon as a direct manifestation of Lifshitz invariant that is allowed in the Ginzburg-Landau free energy when space-inversion and time-reversal symmetries are broken. As demonstrated in our experiment [1], elliptic squeezing of vortices---an inherent property of the non-centrosymmetric superconducting condensate---provides an access to fundamentally new property of Rashba superconductors, and offers an entirely novel approach to vortex manipulation.
Another interesting feature of the non-centrosymmetric superconductors in the applied magnetic field is the supercurrent diode effect---the critical current in one direction exceeds its counterpart in the opposite one---what stems from the Cooper pairs with finite centre of mass momentum. In the pioneering experiment [2] we demonstrated the emergence of the supercurrent diode effect in the Josephson junctions based on synthetic Rashba superconductors made of Al-InAs quantum wells. In the talk, I will discuss a novel experimental method---measurements of the Josephson inductance---and the semiquantitative microscopic model capturing all the essential features as observed in the experiment.

REFERENCES

[1] L. Fuchs, D. Kochan, C. Baumgartner, S. Reinhardt, S. Gronin, G. Gardner, T. Lindemann, M. Manfra, C. Strunk, N. Paradiso; Physical Review X 12 (4), 041020 (2022).
[2] C. Baumgartner, L. Fuchs, A. Costa, S. Reinhardt, S. Gronin, G. Gardner, T. Lindemann, M. Manfra, P. Faria Junior, D. Kochan, J. Fabian, N. Paradiso, C. Strunk; Nature Nanotechnology 17 (1), 39 (2022).

Acta Microscopica Vol. 32, Supp. 1, 2023, pp. xx
PROCEEDINGS NSSY 2023- Galapagos 23th-29th April 2023

FIGURES

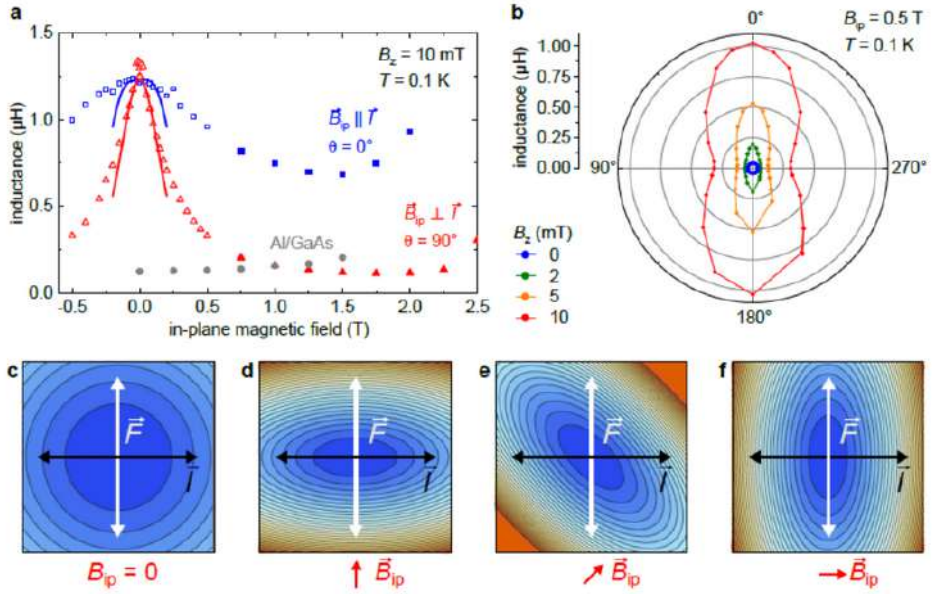

Figure 1. a, Sample inductance of Rashba superconductor as a function of in-plane magnetic field for different orientations of the driving current (red and blue symbols). The controlled measurement (grey symbols) corresponds to a centrosymmetric (i.e. non-Rashba) superconductor. b, Polar plot showing the angle dependence of the vortex inductance for selected values of out-of-plane magnetic field. c, The color plot schematically represents the modulus of the order parameter, $|\psi(x,y)|2$, near the core of a pinned vortex, in the absence of an in-plane field. The horizontal black arrow represents the direction of a current bias, while the white arrow indicates the direction at which a Lorentz force acts on a pinned vortex. The measured vortex inductance is rotation symmetric and inversely proportional to the curvature of $|\psi(x,y)|2$ along the force direction. d-f, When a finite in-plane field is applied the vortex core is squeezed as a consequence of the Rashba spin-orbit interaction, reflecting the measured change in vortex inductance. The curvature is always probed along the white axis, rotating the in-plane magnetic field the vortex rotates keeping its small elliptic axis parallel with the direction of the in-plane field. This allows one to extract from the vortex inductance the spatial profile –order parameter tomography--of $|\psi(x,y)|2$

.

FRIDAY

Theory and Simulations in Nanoscience

Acta Microscopica Vol. 32, Supp. 1, 2023, pp. xx
PROCEEDINGS NSSY 2023- Galapagos 23th-29th April 2023

SPINTERFACE EFFECTS IN ELECTRON TRANSPORT IN CHIRAL MOLECULAR JUNCTIONS

Vladimiro Mujica (1)

(1) Arizona State University, School of Molecular Sciences, Tempe, AZ 85287, U.S.A
vmujica@asu.edu

The term spinterface was coined in spintronics and refers to changes in the interfacial and surface electric and magnetic moments due to spin polarization effects. Spinterface has been proven to be an important element in understanding magnetoresistive effects in single molecule-junctions and it also plays an essential role in triggering the spin polarization response associated with the Chiral-Induced Spin Selectivity (CISS) effect. In this contribution, I will explore the fundamentals of spinterface and how it affects spin polarization and electron transport in chiral interfaces. I will specifically consider the case of a nano-junction consisting of two electrodes (one of them magnetic) and a chiral molecular bridge. The description of spin-polarized transport requires the explicit inclusion of spin-orbit interaction, and the breaking of space-inversion and time-reversal symmetries. The former is associated with chirality, whereas the latter requires the consideration of the molecule as an open system. Furthermore, the analysis of the experimental results in these single-molecule devices explicitly requires the inclusion of spinterface effects to account for the observed asymmetry in the conductance and spin polarization effects, which is the main objective of our study.

REFERENCES

[1] Clarice D. Aiello, John M. Abendroth, Muneer Abbas, Andrei Afanasev, Shivang Agarwal, Amartya S. Banerjee, David N. Beratan, Jason N. Belling, Bertrand Berche, Antia Botana, Justin R. Caram, Giuseppe Luca Celardo, Gianaurelio Cuniberti, Aitzol Garcia-Etxarri, Arezoo Dianat, Ismael Diez-Perez, Yuqi Guo, Rafael Gutierrez, Carmen Herrmann, Joshua Hihath, Suneet Kale, Philip Kurian, Ying-Cheng Lai, Tianhan Liu, Alexander Lopez, Ernesto Medina, Vladimiro Mujica, Ron Naaman, Mohammadreza Noormandipour, Julio L. Palma, Yossi Paltiel, William Petuskey, João Carlos Ribeiro-Silva, Juan José Saenz, Elton J. G. Santos, Maria Solyanik-Gorgone, Volker J. Sorger, Dominik M. Stemer, Jesus M. Ugalde, Ana Valdes-Curiel, Solmar Varela, David H. Waldeck, Michael R. Wasielewski, Paul S. Weiss, Helmut Zacharias, and Qing Hua Wang. A Chirality-Based Quantum Leap, ACS Nano 2022 16 (4), 4989-5035 DOI: 10.1021/acsnano.1c01347

[2] Albert C Aragonès, Ernesto Medina, Miriam Ferrer‐Huerta, Nuria Gimeno, Meritxell Teixidó, Julio L Palma, Nongjian Tao, Jesus M Ugalde, Ernest Giralt, Ismael Díez‐Pérez, Vladimiro Mujica
"Measuring the Spin Polarization Power of a Single Chiral Molecule", Small 13(2017)1602519.

[3] Aragonès AC, Aravena D, Ugalde JM, Medina E, Gutierrez R, Ruiz E, Mujica V, Díez-Pérez I. Magnetoresistive single-molecule junctions: The role of the spinterface and the CISS effect. Isr J Chem [Internet]. 2022;62(11-12)

ACKNOWLEDGMENTS

V.M acknowledges the support of the W. M. Keck Foundation through the grant **Chirality, Spin Coherence and Entanglement in Quantum Biology.**

Acta Microscopica Vol. 32, Supp. 1, 2023, pp. xx
PROCEEDINGS NSSY 2023- Galapagos 23th-29th April 2023

CHIRALLY INDUCED SPIN SELECTIVITY: POLARIZATION FROM DECOHERENCE

Ernesto Medina (1), Solmar Varela (2), Mayra Peralta (4) Bertrand Berche (5), Vladimiro Mujica

(1)Departamento de Física, Universidad San Francisco de Quito, Quito, Ecuador (2) Institute of Materials Science and Nanotechnology, TU Dresden, Germany (3) School of Molecular Sciences, Tempe, Arizona, USA (4) Institute for Material Science, TU Dresden, Germany (5) Laboratoire de Physique et Chimie Theorique, University of Lorraine, Nancy, France.
emedina@usfq.edu.ec

Chirally induced spin selectivity (CISS) has been an intriguing topic of research for almost two decades now and in spite of all the astonishing. experimental manifestations and applications, it has still not completely yielded a complete theory. The experimental evidence of a strong spin selective effect in mostly organic molecules such as individual DNA, Oligopeptides, Proteins, amino acids, helicene, Photosystem I[1], and carbon nanotubes, among many other point chiral and helical structures or chirally connected structures[2]. Two major experimental setups are generally realized: i) Photoelectrons transiting through chiral self-assembled monolayers (SAMS) spin-polarized perpendicular to the SAM surface and ii) STM-Junctions, where electrons transit a single molecule, and spin is injected into a metal or a ferromagnet. In both setups, astonishing polarizations of up to 60%[3,4] are observed, superior to those that can be produced by ferromagnets, albeit in different time scales. In this work, we briefly discuss our group's contributions that have become permanent building blocks in understanding the CISS effect and some of the questions that linger in the problem. We will restrict our discussion to the STM-junction measurements, which most clearly define a single-molecule effect and the transport configuration as a two-terminal problem. In the first theoretical models, the spin-orbit coupling (SOC was surmised to be the spin-active ingredient since no sources of exchange interactions could reasonably be identified in the organic molecules in which the effect is observed. Nevertheless, the source of the coupling was a mystery since the effect's large size seems to require a large SOC in the eV range. We identified early on that this would entail huge electric fields that are not found in the physical system, not even in the atomic nuclei, which result in the well-known relativistic corrections to the atomic spectrum. It was settled going forward that the intrinsic SO coupling of the atoms involved is in the units to tens of meV range at most. In most tight-binding models, this produced only very small transport polarizations, although much larger than those of classical gas phase experiments for point chiral molecules. A very elegant way to see the material sources of the SOC is by thinking of long molecules as quasi-one-dimensional solids and using the k.p argument in a Hamiltonian that includes SOC.

Taking into account the electron filling of the mobile electron orbitals and using the wave functions of that filling as a basis, one can show that the SOC comes from the electric fields of the atomic nuclei, and the momenta involved are those of the electron clouds of the molecular component atoms where the SOC enters

$$\Delta_{\cdot\,\cdot\,\cdot\,\cdot} = (\hbar^2/4m_0^2c^2)\langle n'\sigma'|\mathbf{p}\cdot\sigma\times(\nabla V_0)|n\sigma\rangle,$$

showing the relevant momenta and field.

$$\sum_{n,\sigma}\left\{\left[E_n(\mathbf{0})+\frac{\hbar^2k^2}{2m_0}\right]\delta_{nn'}\delta_{\sigma\sigma'}+\frac{\hbar}{m_0}\mathbf{k}\cdot\mathbf{P}_{nn'\sigma\sigma'}+\langle\langle V(r)\rangle\rangle+\Delta_{nn'\sigma\sigma'}\right\}c_{\nu n\sigma}(\mathbf{k})=E_\nu(\mathbf{k})|c_{\nu n'\sigma'}(\mathbf{k})\rangle$$

gradients are those expected from the local orbitals while referring only to kinetic quantities[5].

Another challenge to theories was related to the two terminal setups and measurement of spin polarization. The work of van Wees et al [6] reminded the community that time reversal symmetric coupling could not polarize spin by itself in two terminal measurements (see also [2]). This is a consequence of the Onsager relations applicable to the linear regime. A natural source of time-reversal symmetry breaking (TRSB) is a third probe that can couple to the electron transport. This can occur via electron-phonon interactions where

Acta Microscopica Vol. 32, Supp. 1, 2023, pp. xx
PROCEEDINGS NSSY 2023- Galapagos 23th-29th April 2023

phonons have a thermal distribution [7] or via a third probe that at least scrambles the phase information of the electrons while preserving unitarity. Also a major problem of previous theoretical models is the assumption of metallic-like transport that does not occur in molecular transport. We addressed both shortcomings in a quasi-one-dimensional Rashba model tunneling under a spin active barrier coupled to a third probe. The model is unitary but includes dephasing effects due to an electron reservoir implemented through a Buttiker probe[8]. As expected, the model does not yield net polarization in the two-terminal setup but yields strong polarizations for meV SO coupling (See Figure 1). The scenario for this effect is that tunneling exponentially enhances the dephasing effects of the third probe in the Safeway a magnetic field under the barrier would work. We believe this model is amenable to coupling to either electron-phonon or electron-electron interactions in contact with a thermal reservoir and would explain spin polarization in the linear regime.

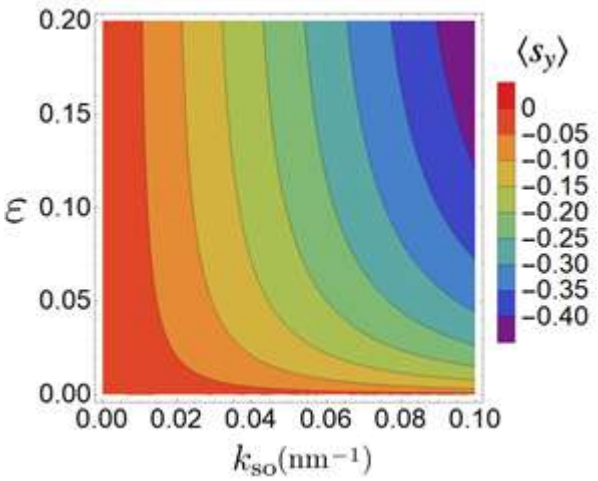

Figure 1: Polarization produced by a decoherence probe (controlled by) coupled to tunneling in a SO active barrier. The color shades represent the generated y component of the spin induced by time reversal symmetry breaking as a function of the spin-orbit strength . A large spin polarization is achieved by the atomic SOC exponentiated by tunneling

Another challenge to theories was related to the two terminal setups and measurement of spin polarization. The work of van Wees et al [6] reminded the community that time reversal symmetric coupling could not polarize spin by itself in two terminal measurements (see also [2]). This is a consequence of the Onsager relations applicable to the linear regime. A natural source of time-reversal symmetry breaking (TRSB) is a third probe that can couple to the electron transport. This can occur via electron-phonon interactions where phonons have a thermal distribution [7] or via a third probe that at least scrambles the phase information of the electrons while preserving unitarity. Also a major problem of previous theoretical models is the assumption of metallic-like transport that does not occur in molecular transport. We addressed both shortcomings in a quasi-one-dimensional Rashba model tunneling under a spin active barrier coupled to a third probe. The model is unitary but includes dephasing effects due to an electron reservoir implemented through a Buttiker probe[8]. As expected, the model does not yield net polarization in the two-terminal setup but yields strong polarizations for meV SO coupling (See Figure 1). The scenario for this effect is that tunneling exponentially enhances the dephasing effects of the third probe in the Safeway a magnetic field under the barrier would work. We believe this model is amenable to coupling to either electron-phonon or electron-electron interactions in contact with a thermal reservoir and would explain spin polarization in the linear regime.

Acta Microscopica Vol. 32, Supp. 1, 2023, pp. xx
PROCEEDINGS NSSY 2023- Galapagos 23th-29th April 2023

REFERENCES

[1] Naaman R, Waldeck D. H. Annu. Rev. Phys. Chem. (2015)(66)(263).
[2] Guo A.-M Phys. Rev. B (2016)(94)(165409).
[3] Gohler B. et al Science (2011)(331)(894).
[4] Xie Z. et al Nano Lett. (2011)(11)(4652).
[5] Winkler R. (2003) *Spin-Orbit Coupling Effects in Two Dimensional Electron and Hole Systems,* Berlin Springer-Verlag.
[6] Yang X. et al Nano Lett. (2020) (20), (6148).
[7] Fransson J. Phys. Rev. B (2020)(102)(235416).
[8] Varela S. et al Arxiv: 2301.02156 (2023).

ACKNOWLEDGMENTS

EM thanks POLI grant POLI 014EM of USFQ for funding and visiting Professorships to the University of Lorraine.

Acta Microscopica Vol. 32, Supp. 1, 2023, pp. xx
PROCEEDINGS NSSY 2023- Galapagos 23th-29th April 2023

AB INITIO STUDIES OF BULK AND (001) SURFACES OF THE METAL HALIDE DOUBLE PEROVSKITE $CS_2AU_2CL_6$

Anthony Vizcaino (1), Henry Pinto (2)

(1) CompNano Group, School of Physical Sciences and Nanotechnology, Yachay Tech University, Urcuqui 100119, Ecuador. (2) CompNano Group, School of Physical Sciences and Nanotechnology, Yachay Tech University, Urcuqui 100119, Ecuador.
anthony.vizcaino@hotmail.com

Perovskites are materials that have gained particular importance in recent years due to their application in the electronics industry, such as semiconductors and piezoelectrics. Furthermore, many materials can be considered perovskites if they have an atomic structure defined by $A_2B_2X_6$. Among all these possibilities, we present the study of $Cs_2Au_2Cl_6$ metal halide double perovskites, which use elements that do not harm the environment and do not produce as much damage as before (lead), aligning our research with the UN sustainable development goals: climate action and affordable, clean energy. This work builds on a previous study of the Integrated experimental and theoretical approach for the efficient design and synthesis of gold-based double-halide perovskites. However, it is considered relevant to deepen the study of this compound to establish a state-of-the-art that complements the previous analyses. We perform Density Functional Theory (DFT) surface calculations using the SCAN functional (Strongly Constrained and Appropriately Normed), 4-layer slab model and vacuum of 15 Å; to determine the electronic properties. We analyzed all the atomic models that this material could have; one terminated in gold and chlorine (model A), the other terminated in chlorine and cesium and chlorine (model B), and we also created models with point defect vacancies by removing chlorine atoms from the surface and subsurface with the objective of manipulate the band gap. The most stable model $Cs_2Au_2Cl_6$ is the surface B, which was determined using the energy of the system, with a difference in energy of 0.10 eV from surface A. We calculated the partial density of states (PDOS), and the results suggest that on the surface, the valence band has contributions of gold and chlorine, which correspond mainly to the Au-d, Cl-p states, and a lesser extent, the cesium contribution belongs to Cs-p states. Meanwhile, the conduction band has gold, chlorine, and cesium contributions with Au-s, Au-d, Cl-p, and Cs-d states. Of all the models presented, only the l4a-2clv, l4b-2clv2B, and l4a are insulators; all other atomic models show metallic behavior in their outermost layer. In addition, we simulated Scanning Tunneling Microscope (STM) images showing that the surface atoms in model A correspond to gold and in model B correspond to chlorine. We also computed Ultraviolet Photoelectron Spectroscopy (UPS) images, and in all models studied, there is a significant contribution from gold and chlorine atoms and a small contribution from cesium. Additionally, the formation of energy vacancies was calculated from where the models (l4b-clvB) and (l4a-clv) are the ones that require less energy to be produced. Finally, we calculate the work function for all the models, (l4a-sclvB) and (l4b-2clv2A), which require less energy. Further DFT work could be done using bromine (Br) or iodine (I) elements instead of chlorine to determine which gold-based double-halide perovskites exhibit the best electronic and mechanical properties.

REFERENCES

[1] Bajorowicz, B.; Mikolajczyk, A.; Pinto, H. P.; Miodynska, M.; Lisowski, W.; Klimczuk, T.; Kaplan-Ashiri, I.; Kazes, M.; Oron, D.; Zaleska-Medynska, A. Integrated experimental and theoretical approach for efficient design and synthesis of gold-based double halide perovskites. The Journal of Physical Chemistry C 2020, 124, 26769–26779

[2] Giustino, F. Materials modelling using density functional theory: properties and predictions; Oxford University Press, 2014

[3] Freysoldt, C.; Grabowski, B.; Hickel, T.; Neugebauer, J.; Kresse, G.; Janotti, A.; Van de Walle, C. G. First-principles calculations for point defects in solids. Reviews of modern physics 2014, 86, 253

ACKNOWLEDGMENTS

My sincere gratitude to my tutor Henry Pinto for being my guide, teacher, and friend during my time at Yachay Tech.

FIGURES

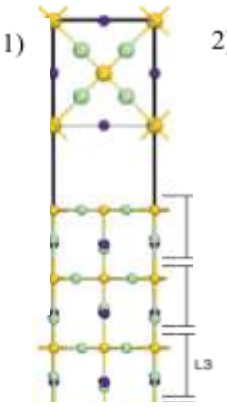

Fig 1. Atomic structure model A

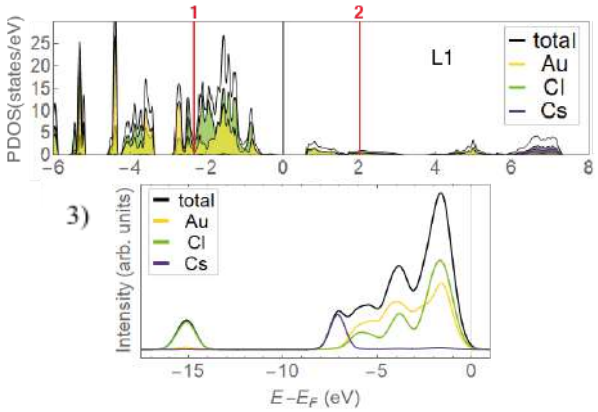

Fig 3. UPS of the surface

SURFACE MODEL A

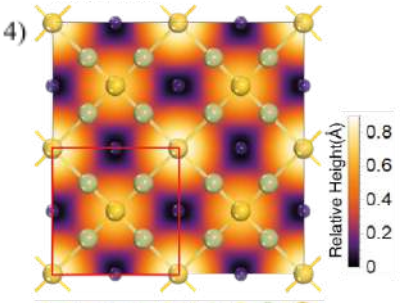

Fig 4. STM and relative height using V_{bias} = -1.10 V

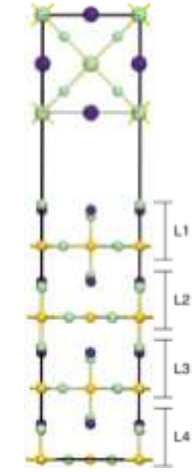

Fig 5. Atomic structure model B

SURFACE MODEL B

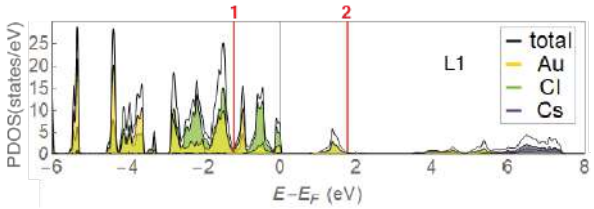

Fig 6. PDOS of the outermost layer

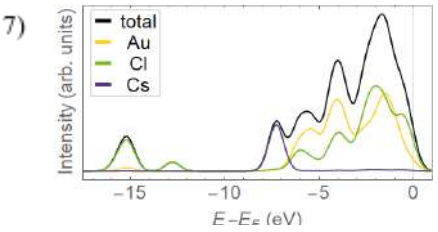

Fig 7. UPS of the surface

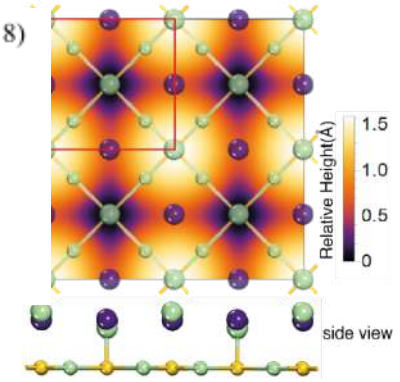

Fig 8. STM and relative height using V_{bias} = -0.85 V

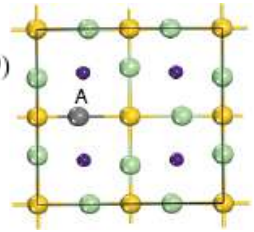

Fig 9. A vacancy for Surface A

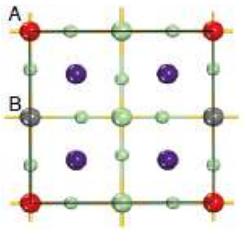

Fig 10. A and B vacancies for Surface B

Table 1. Results summary. Vacancy type, behavior, work function (ϕ), and energy vacancy formation.

Vacancy Type	Behaviour	ϕ (eV)	Energy Formation(eV)
l4a-clv	metallic	6.31	16.26
l4a-2clv	insulator	6.74	24.83
l4a-sclvA	metallic	6.96	16.39
l4a-sclvB	metallic	6.28	17.88
l4b-clvA	metallic	4.68	18.29
l4b-clvB	metallic	3.54	17.20
l4b-2clv2A	metallic	2.31	35.33
l4b-2clv2B	insulator	3.89	34.62

Acta Microscopica Vol. 32, Supp. 1, 2023, pp. xx
PROCEEDINGS NSSY 2023- Galapagos 23th-29th April 2023

COLLECTIVE VIBRATIONS IN HOMOGENEOUS CARBON NANOTUBE BUNDLES

Charlotte Berrezueta-Palacios(1), Dekel Nakar(2), Anna Wroblewska(3), Oisín Garrity(1), Han Li(4), Benjamin Scott Flavel(4), Ernesto Joselevich(2), Stephanie Reich(1) and Georgy Gordeev(1, 5)
(1) Department of Physics, Freie Universität Berlin, Berlin 14195,Germany. (2) Department of Materials and Interfaces, Weizmann Institute of Science, Rehovot 7610001, Israel. (3) Faculty of Physics, Warsaw University of Technology,

Koszykowa 75, 00-662, Warsaw, Poland. (4) Institute of Nanotechnology, Karlsruhe Institute of TechnologyHermann-von-Helmholtz-Platz 1, 76344 Eggenstein-Leopoldshafen, Germany. (5) Department of Physics and Materials Science, University of Luxembourg, L-4422 Belvaux, Luxembourg.
charlotte.berrezueta@fu-berlin.de

Carbon nanotubes (CNTs) are tiny hollow cylinders made of carbon. Raman spectroscopy is one of the most widespread techniques for the analysis of CNT, as it can identify their microscopic structure. In particular, much attention is paid to the low frequency region where the radial breathing mode (RBM) peak is observed. Because of their curved structure, RBM peak arises as a unique spectral feature from CNTs it describes the breathing-like behavior originating from the symmetric vibration in a radial direction with respect to the tube axis. For isolated tubes, a single peak is observed with a frequency that is inversely proportional to the tube's diameter. The physical properties of individual CNTs differ from the CNT bundles, aggregated CNT form and are regulated by its chiral purity and degree of bundling. The higher-dimensional arrangement of nanomaterials materials can influence their vibrational modes. When identical CNTs get arranged into Two-dimensional hexagonal lattices, their vibrational properties were predicted to change and additional low-frequency modes were expected in the Raman spectrum arising from collective vibrations [1]. However, the experimental study of collective vibrations has been limited due to the difficulty in obtaining homogeneous chirality bundles. To observe these collective vibrational features, one must measure high-quality single chirality bundles which are still a current challenge in synthesis processes. There are two approaches that can create homogeneous aggregations of nanotubes: a solution based on a CNT solution vacuum filtration and direct coiling during CVD growth. Both approaches in principle can yield extremely pure material. Here, we present a Raman study of the collective vibrational modes arising from homogeneous bundles formed by a SWCNT coil and a homogeneous carbon nanotube film. Through a self-coiling mechanism, carbon nanotubes can be arranged into coils after grown during their synthesis process and comprise perfectly aligned homologous bundles with a radial shape. By characterizing and comparing the physical properties of the coil with respect to its ends, the bundling effects can be isolated and studied[2,3]. In such structures we observe two breathing-like modes RBM(B1) and RBM(B2) in contrast to the single radial breathing mode characteristic for isolated tubes. We investigate the exciton-phonon coupling for these modes with resonant Raman spectroscopy finding the same resonance energy for both BM peaks and confirming that both modes originate from the same chirality bundle. Additionally, we study the tube's diameter dependence of vibrational coupling by analyzing different tube's diameter coils and film samples. We compare our experimental findings with theoretical lattice-dynamical study of infinite bundles of identical tubes accomplished within a valence force field (VVF) model with intertube interactions described by a Lennard Jones potential. These results provide an insight into intra-tube lattice dynamics in carbon nanotubes bundles for better understanding of collective vibrational effects.

REFERENCES

[1] Popov, V.N.et al. Physical Review B, (2001) 63(23), p.233407.
[2] Shadmi, N. et al. 2016, 16(4), pp.2152-2158.
[3] Nakar, Det et al. 2019. Nano Letters, 20(2), pp.953-962.

Acta Microscopica Vol. 32, Supp. 1, 2023, pp. xx
PROCEEDINGS NSSY 2023- Galapagos 23th-29th April 2023

FIGURES

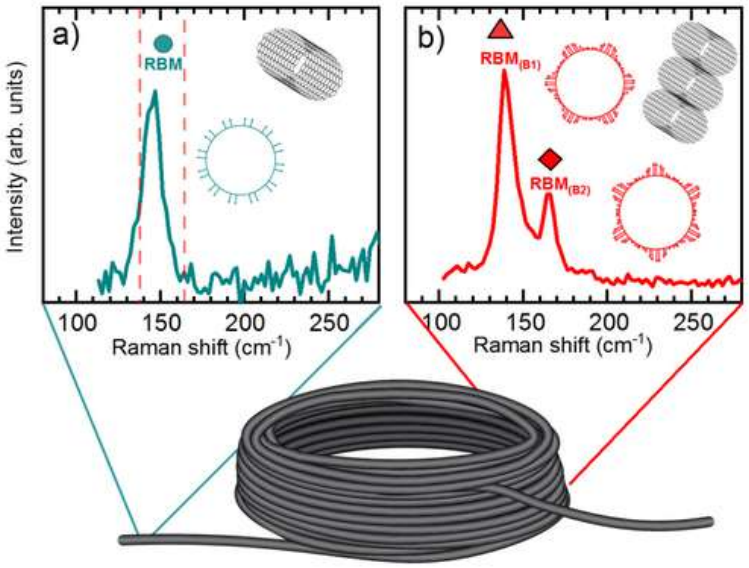

Figure1. Raman spectroscopy of the Radial breathing modes of carbon nanotube coil. a) Raman spectra for tail and b) coil (isolated vs bundles effects). The peaks originating from collective vibrations are observed by RBM(B1) and RBM(B2).

Acta Microscopica Vol. 32, Supp. 1, 2023, pp. xx
PROCEEDINGS NSSY 2023- Galapagos 23th-29th April 2023

DISCLOSING THE OPTICAL PROPERTIES OF SINGLE CHIRALITY SORTED SINGLE-WALLED CARBON NANOTUBES

Joselyn Benalcázar [1], Dido Denier van der Gon [1], Yohei Yomogida [2], Kazuhiro Yanagi [2], and Paola Ayala[1]

1 University of Vienna, Faculty of Physics, Boltzmanngasse 5, 1090 Vienna, Austria
2 Tokyo Metropolitan University, Department of Physics, Minami-Osawa 1-1, 1920397, Tokyo, Japan
joselyn.benalcazar@univie.ac.at

Understanding the optical properties of single-walled carbon nanotubes (SWCNTs) is of major interest to bring their applicability in optoelectronics, photonic and bioimaging to reality. From the theoretical point of view, several predictions have shown that the physical properties of SWCNTs depend on the geometrical configuration of the carbon atoms that construct their walls. This implies a definition for the chiral vector, chiral angle and consequently the chiral indexes (n,m). However, from the experimental point of view, observing those predicted properties imposes challenges that still embrace the production of the nanotube-material. For each specific chirality, defined and unique optical transitions are expected. These can be nicely identified with methods like optical absorption and Raman spectroscopy, and this has been done even in chirality mixed samples given that a reasonable debundling is achieved. Nevertheless, every foreign chirality in a batch represents an impurity. For that reason, it is extremely important to produce chirality sorted samples. For many years now, various methods have been developed. Among these, gel chromatography has been very successful to produce high yield and high purity samples at large scale quantities. This method is based on the selective adsorption of surfactants with different hydrophobicity on the nanotube´s surface at given adsorption sites, while leaving others free to stick in the gel for further gradient elution. Therefore, a careful load of surfactants and a controlled flow of the nanotubes through the gel are key parameters to explore how to increase the purity of single chirality sorting experiments. Chirality species are otherwise obtained after second purification processes in which most of them use surfactants to separate nanotubes by electronic character, diameter or chirality. In this work, we show a full optical characterization of single-chirality sorted SWCNTs processed by a modified gel chromatography process where the temperature dependence plays a crucial role. The preferential adsorption mechanism of the surfactants with different hydrophobicities onto the nanotubes' surface is shown. We focus on how their diameter and chirality can be correlated with a controlled-flow that involves a careful monitoring of the temperature.. The (10,0) zig-zag chirality will be used as an example of how a single chirality sample can be obtained in a 2 step process. Additionally, first results of high purity (11,0) chirality sorting are shown.